

Non-adiabatic ring polymer molecular dynamics in the phase space of the $SU(N)$ Lie group

Cite as: J. Chem. Phys. **158**, 044123 (2023); <https://doi.org/10.1063/5.0133970>

Submitted: 07 November 2022 • Accepted: 08 January 2023 • Accepted Manuscript Online: 10 January 2023 • Published Online: 31 January 2023

 [Duncan Bossion](#),  [Sutirtha N. Chowdhury](#) and  [Pengfei Huo](#)



[View Online](#)



[Export Citation](#)



[CrossMark](#)

ARTICLES YOU MAY BE INTERESTED IN

[Non-adiabatic mapping dynamics in the phase space of the \$SU\(N\)\$ Lie group](#)

The Journal of Chemical Physics **157**, 084105 (2022); <https://doi.org/10.1063/5.0094893>

[Non-adiabatic ring polymer molecular dynamics with spin mapping variables](#)

The Journal of Chemical Physics **154**, 184106 (2021); <https://doi.org/10.1063/5.0051456>

[Theory of vibrational polariton chemistry in the collective coupling regime](#)

The Journal of Chemical Physics **156**, 014101 (2022); <https://doi.org/10.1063/5.0074106>

[Learn More](#)

The Journal of Chemical Physics **Special Topics** Open for Submissions

Non-adiabatic ring polymer molecular dynamics in the phase space of the $SU(N)$ Lie group

Cite as: J. Chem. Phys. 158, 044123 (2023); doi: 10.1063/5.0133970

Submitted: 7 November 2022 • Accepted: 8 January 2023 •

Published Online: 31 January 2023



View Online



Export Citation



CrossMark

Duncan Bossion,^{1,a)} Sutirtha N. Chowdhury,¹ and Pengfei Huo^{1,2,b)}

AFFILIATIONS

¹ Department of Chemistry, University of Rochester, 120 Trustee Road, Rochester, New York 14627, USA

² The Institute of Optics, Hajim School of Engineering, University of Rochester, Rochester, New York 14627, USA

^{a)} Electronic mail: dbossion@ur.rochester.edu

^{b)} Author to whom correspondence should be addressed: pengfei.huo@rochester.edu

ABSTRACT

We derive the non-adiabatic ring polymer molecular dynamics (RPMD) approach in the phase space of the $SU(N)$ Lie Group. This method, which we refer to as the spin mapping non-adiabatic RPMD (SM-NRPMD), is based on the spin-mapping formalism for the electronic degrees of freedom (DOFs) and ring polymer path-integral description for the nuclear DOFs. Using the Stratonovich–Weyl transform for the electronic DOFs and the Wigner transform for the nuclear DOFs, we derived an exact expression of the Kubo-transformed time-correlation function (TCF). We further derive the spin mapping non-adiabatic Matsubara dynamics using the Matsubara approximation that removes the high frequency nuclear normal modes in the TCF and derive the SM-NRPMD approach from the non-adiabatic Matsubara dynamics by discarding the imaginary part of the Liouvillian. The SM-NRPMD method has numerical advantages compared to the original NRPMD method based on the Meyer–Miller–Stock–Thoss (MMST) mapping formalism due to a more natural mapping using the $SU(N)$ Lie Group that preserves the symmetry of the original system. We numerically compute the Kubo-transformed position auto-correlation function and electronic population correlation function for three-state model systems. The numerical results demonstrate the accuracy of the SM-NRPMD method, which outperforms the original MMST-based NRPMD. We envision that the SM-NRPMD method will be a powerful approach to simulate electronic non-adiabatic dynamics and nuclear quantum effects accurately.

Published under an exclusive license by AIP Publishing. <https://doi.org/10.1063/5.0133970>

I. INTRODUCTION

Accurately simulating the quantum dynamics of molecular systems in condensed phase remains a challenge in theoretical chemistry due to the difficulties of accurately describing electronically non-adiabatic dynamics and nuclear quantum effects.¹ Such effects are inherent to a lot of key reactions in biochemistry, catalysis, and energy applications that involve electron transfer or proton-coupled electron transfer processes.^{2–4} Despite the recent progress on new theoretical approaches to study those types of reactions, the challenge remains for large systems with many degrees of freedom (DOFs), and the exact quantum simulations remain computationally expensive due to the unfavorable numerical scaling.

Recently emerged state-dependent ring-polymer molecular dynamics (RPMD) approaches provide a unified description of both the electronically non-adiabatic dynamics and nuclear quantum effects using a trajectory-based description. Ring-polymer molecular dynamics (RPMD)^{5–9} based on Feynman’s imaginary-time

path-integral formalism was originally developed for electronically adiabatic systems to effectively capture the nuclear quantum effects through extended phase space quantization. State-dependent RPMD methods are developed based on the RPMD framework, aiming to provide both accurate non-adiabatic dynamics with an explicit description of electronic states and reliable treatment of nuclear quantum dynamics through the ring polymer path-integral quantization. These methods include mean-field RPMD,¹⁰ non-adiabatic RPMD (NRPMD),^{11–13} mapping variable RPMD (MV-RPMD),^{14–16} ring-polymer Ehrenfest dynamics,¹⁷ kinetically constrained RPMD (KC-RPMD),^{18,19} coherent state RPMD (CS-RPMD),²⁰ and ring-polymer surface hopping (RPSH),^{21–24} to name a few.

Among these various state-dependent RPMD approaches, NRPMD^{11–13,25} provides both accurate nuclear quantum dynamics and accurate electronic Rabi oscillations, thus being an ideal approach to investigate quantum dynamics of non-adiabatic

systems.^{13,26} This approach is based on the Meyer–Miller–Stock–Thoss (MMST) mapping formalism^{27–29} and has been formally derived using the non-adiabatic Matsubara dynamics formalism in our previous work.²⁵ The non-adiabatic Matsubara dynamics formalism²⁵ also uses the MMST mapping representation, which can be viewed as the state-dependent generalization of the Matsubara dynamics framework by Althorpe and co-workers.^{30,31}

The MMST mapping formalism,^{27–29} despite its great success and broad applications,^{11,12,32–38} has known flaws.^{39–41} In particular, it maps a N -level system onto N singly excited harmonic oscillators (SEO), resulting in mapping variables that are the conjugate position and momentum of each oscillator. This leads to a symmetry $\otimes_N \mathfrak{su}(2)$ for the mapped system as each harmonic oscillator in this subspace has a symmetry $\mathfrak{su}(2)$ (only the ground and first excited states of the oscillators belong to the SEO subspace), whereas the original symmetry of a N -level system should be $\mathfrak{su}(N)$. Due to this mapping procedure, the MMST mapping operators belong to a larger Hilbert space that contains states outside the SEO subspace, whereas the MMST mapping procedure tries to map the original electronic subspace onto the SEO subspace. It thus requires a projection back to the SEO subspace to obtain accurate results.^{39–41} As a consequence, the identity operator is not preserved through the MMST mapping, and there is an ambiguity on how to evaluate it.⁴¹ Related to the problem of the non-conserving identity, the non-adiabatic dynamics is sensitive to the separation between the state-dependent and the state-independent Hamiltonian.^{40,42}

Recently, a new mapping formalism based on the phase space of the $SU(N)$ Lie Group has been proposed by Runeson and Richardson.^{43,44} This new mapping formalism, referred to as the generalized spin mapping, preserves the original $\mathfrak{su}(N)$ symmetry of the Hamiltonian. Runeson and Richardson used the spin operators [which are equivalent to the generators of the $\mathfrak{su}(N)$ Lie algebra up to a constant] and the $SU(N)$ Lie group to perform the non-adiabatic mapping dynamics of a N -state vibronic Hamiltonian and developed the spin-Linearized semi-classical (spin-LSC) approach.⁴⁴ In particular, the Stratonovich–Weyl (SW) transform^{45–48} is used to map an operator in the Hilbert space described by the spin operators to a continuous function on the Lie group/manifold, resulting in a classical-like Hamiltonian. The SW transform evaluates the expectation values of the spin operators under the generalized spin coherent states (SCS).^{49,50} We have also provided a detailed derivation of the quantum Liouvillian and the linearized Liouvillian based on the spin mapping framework.⁵¹ Based on the $SU(2)$ Lie group, we have proposed a spin mapping NRPMD dynamics approach⁵² for two-level systems ($N = 2$), purely based on the standard path-integral derivation, which is based on a partition function.

In this work, we apply the spin mapping formalism to describe the electronic DOFs and Wigner representation for the nuclear DOFs and derive the expression of the exact Kubo-transformed time correlation function (TCF). Applying the Matsubara approximation³⁰ and ring polymer approximation³¹ to this exact TCF leads to the spin-mapping NRPMD (SM-NRPMD) method. With the spin mapping formalism respecting the symmetry of the original system, the SM-NRPMD approach explicitly addresses the limitations of the NRPMD method¹¹ due to the deficiencies of the MMST mapping formalism. The outline of this paper is described as follows: In Sec. II, a brief overview of the $SU(N)$ mapping formalism is provided, together with the procedure to map a general operator

in the electronic and nuclear Hilbert space through a mixed Stratonovich–Weyl/Wigner transformation. In Sec. III, we provide an exact expression of the Kubo-transformed TCF and the corresponding exact quantum Liouvillian. In Sec. IV, we introduce the Matsubara approximation and the RPMD approximation, upon which we derive the SM-NRPMD correlation function. The accuracy of the SM-NRPMD method is tested using three-level systems in Secs. V and VI and compared to the MMST-based NRPMD approach,¹¹ demonstrating a significant improvement due to the spin mapping formalism. The conclusions and future directions are provided in Sec. VII.

II. THE $SU(N)$ MAPPING FORMALISM

In this section, we briefly outline the basic idea of the $SU(N)$ mapping formalism, where the details can be found in the previous works.^{44,51} We are interested in the quantum dynamics of a system of N electronic states coupled to nuclear DOFs as follows:

$$\begin{aligned}\hat{H} &= [\hat{T}_R + U_0(\hat{R})] \otimes \hat{\mathcal{I}} + \hat{V}_e(\hat{R}) \\ &= [\hat{T}_R + U_0(\hat{R})] \otimes \hat{\mathcal{I}} + \sum_{n,m} V_{nm}(\hat{R}) |n\rangle\langle m|,\end{aligned}\quad (1)$$

where \hat{T}_R is the nuclear kinetic energy operator, $U_0(\hat{R})$ represents the state-independent part of the potential, and $\hat{V}_e(\hat{R})$ is the state-dependent part of the potential. While we consider one nuclear DOF \hat{R} for convenience, the theory in this work can be easily generalized to many nuclear DOFs. Furthermore, $\{|n\rangle\}$ represents a set of diabatic electronic states, and $V_{nm}(\hat{R}) = \langle n|\hat{V}_e(\hat{R})|m\rangle$ is the matrix element of $\hat{V}_e(\hat{R})$ in this diabatic representation. The electronic identity operator $\hat{\mathcal{I}} = \sum_{n=1}^N |n\rangle\langle n|$ represents the identity in the electronic Hilbert space. Note that this is a rather general Hamiltonian, representing a quantum subsystem that has N states coupled to a “classical” subsystem.

We aim to evaluate the TCF governed by the Hamiltonian in Eq. (1). In Secs. II A–II C, we use the $SU(N)$ mapping formalism to map discrete electronic states onto continuous variables in the $SU(N)$ phase space and the Wigner representation to describe the nuclear DOFs. The detailed derivation of all expressions can be found in our previous work in Ref. 51. This mixed representation will be used to express the Kubo-transformed TCF in Sec. IV.

A. The spin mapping formalism in the $SU(N)$ representation

We briefly review the general expressions of the generators of the $\mathfrak{su}(N)$ Lie algebra, which will be used as a matrix basis to represent electronic operators. The commutation (and anti-commutation) relations among these generators are defined in the $\mathfrak{su}(N)$ Lie algebra, whereas the exponential functions of these generators construct the elements of the $SU(N)$ Lie group via the exponential map.^{53,54}

The generators, denoted as \hat{S}_i , are expressed in Appendix A. These generators are traceless, $\text{Tr}_e[\hat{S}_i] = 0$, and are orthonormal to each other as $\text{Tr}_e[\hat{S}_i \hat{S}_j] = \frac{\hbar^2}{2} \delta_{ij}$. The commutation and anti-commutation relations among the generators of the $\mathfrak{su}(N)$ Lie algebra are presented as follows:

$$[\hat{S}_i, \hat{S}_j] = i\hbar \sum_{k=1}^{N^2-1} f_{ijk} \hat{S}_k, \quad (2a)$$

$$\{\hat{S}_i, \hat{S}_j\}_+ = \frac{\hbar^2}{N} \delta_{ij} \hat{\mathcal{I}} + \hbar \sum_{k=1}^{N^2-1} d_{ijk} \hat{S}_k, \quad (2b)$$

where $\{\hat{S}_i, \hat{S}_j\}_+$ represents the anti-commutator between \hat{S}_i and \hat{S}_j and f_{ijk} and d_{ijk} are the totally anti-symmetric and totally symmetric *structure constants*, respectively. Using Eqs. (2a) and (2b), one can express the structure constants as

$$f_{ijk} = -i \frac{2}{\hbar^3} \text{Tr}[[\hat{S}_i, \hat{S}_j] \hat{S}_k], \quad (3a)$$

$$d_{ijk} = \frac{2}{\hbar^3} \text{Tr}[\{\hat{S}_i, \hat{S}_j\}_+ \hat{S}_k]. \quad (3b)$$

The generators of an algebra $\{\hat{S}_k\}$ can be obtained in different ways, but the most commonly used ones are based on a generalization of the Pauli matrices of $\mathfrak{su}(2)$ and of the Gell-Mann matrices⁵⁵ of $\mathfrak{su}(3)$, which is what is used in this work. This representation of the generators is referred to as the Generalized Gell-Mann matrix (GGM) basis.^{56,57} Their detailed expressions are provided in Appendix A [see Eqs. (A1)–(A3)]. One can also derive an analytic expression (closed formulas) of f_{ijk} and d_{ijk} for the GGM basis, which can also be found in Appendix A. The derivation of them can be found in our previous work in Ref. 51.

Using these generators, the Hamiltonian \hat{H} [Eq. (1)] is represented as follows:^{44,58}

$$\hat{H} = \mathcal{H}_0(\hat{R}, \hat{P}) \cdot \hat{\mathcal{I}} + \frac{1}{\hbar} \sum_{k=1}^{N^2-1} \mathcal{H}_k(\hat{R}) \cdot \hat{S}_k, \quad (4)$$

where the elements $\mathcal{H}_0(\hat{R}, \hat{P})$ and $\mathcal{H}_k(\hat{R})$ are expressed as

$$\mathcal{H}_0(\hat{R}, \hat{P}) = \frac{1}{N} \text{Tr}_{\text{e}}[\hat{H} \cdot \hat{\mathcal{I}}] = \hat{T}_R + U_0(\hat{R}) + \frac{1}{N} \sum_{n=1}^N V_{nn}(\hat{R}), \quad (5a)$$

$$\mathcal{H}_k(\hat{R}) = \frac{2}{\hbar} \text{Tr}_{\text{e}}[\hat{H} \cdot \hat{S}_k] = \frac{2}{\hbar} \text{Tr}_{\text{e}}[\hat{V}_{\text{e}}(\hat{R}) \cdot \hat{S}_k]. \quad (5b)$$

Note that Eq. (5) has an explicit separation of the trace and traceless parts of the potential due to the traceless definition of the generators. Furthermore, we can explicitly write $\mathcal{H}_k(\hat{R})$ in Eq. (5b) as

$$\mathcal{H}_{\alpha_{nm}}(\hat{R}) = V_{mn}(\hat{R}) + V_{nm}(\hat{R}), \quad (6a)$$

$$\mathcal{H}_{\beta_{nm}}(\hat{R}) = i(V_{mn}(\hat{R}) - V_{nm}(\hat{R})), \quad (6b)$$

$$\mathcal{H}_{\gamma_n}(\hat{R}) = \sum_{l=1}^{n-1} \sqrt{\frac{2}{n(n-1)}} V_{ll}(\hat{R}) - \sqrt{\frac{2(n-1)}{n}} V_{nn}(\hat{R}), \quad (6c)$$

where $\alpha_{nm} = n^2 + 2(m-n) - 1$ is the index related to the symmetric non-diagonal generators, $\hat{S}_{\alpha_{nm}}$ [Eq. (A1)], $\beta_{nm} = n^2 + 2(m-n)$ is the index related to the asymmetric non-diagonal generators, $\hat{S}_{\beta_{nm}}$ [Eq. (A2)], and $\gamma_n = n^2 - 1$ is the index related to the diagonal generators \hat{S}_{γ_n} [Eq. (A3)], with $1 \leq m < n \leq N$ and $2 \leq n \leq N$.

B. The Stratonovich-Weyl transform

The Stratonovich-Weyl (SW) transform evaluates the expectation values of the spin operators under the generalized spin coherent states.^{49,50} The generalized spin coherent states are expressed as

$$|\Omega\rangle = \sum_{n=1}^N |n\rangle \langle n|\Omega\rangle, \quad (7)$$

where the detailed expression of the expansion coefficients, $\langle n|\Omega\rangle$, are provided in Eq. (B1). The spin coherent states are normalized, $\langle \Omega|\Omega\rangle = 1$, and they form a resolution of identity,^{50,57,59,60}

$$\hat{\mathcal{I}} = \sum_n |n\rangle \langle n| = \int d\Omega |\Omega\rangle \langle \Omega|, \quad (8)$$

where the expression of the differential phase-space volume element $d\Omega \equiv \mathbf{K}(\theta) d\theta d\varphi$ is provided in Eq. (B2) in terms of the $2N - 2$ independent variables, $\{\theta, \varphi\}$, which are the generalized Euler angles of the N -dimensional Bloch sphere. In the following, we define the expectation value of the generalized spin operators as

$$\hbar\Omega_k \equiv \langle \Omega|\hat{S}_k|\Omega\rangle, \quad (9)$$

where $\hbar\Omega$ plays the role of the Bloch vector^{61,62} and is referred to as the generalized Bloch vector.^{61,62} Its detailed expression in terms of $\{\theta, \varphi\}$ is provided in Eqs. (B5)–(B7).

The SW transform of an operator \hat{A} is defined as

$$[\hat{A}]_s(\Omega) = \text{Tr}_{\text{e}}[\hat{A} \cdot \hat{w}_s], \quad (10)$$

where \hat{w}_s is the kernel of the SW transform, with the following expression:^{47,57,63}

$$\hat{w}_s(\Omega) = \frac{1}{N} \hat{\mathcal{I}} + r_s \cdot \frac{2}{\hbar} \sum_{i=1}^{N^2-1} \Omega_i \cdot \hat{S}_i. \quad (11)$$

The parameter r_s is related to the radius of the Bloch sphere^{64–66} representing the electronic states of the system. The kernel also defines an identity as follows:

$$\int d\Omega \hat{w}_s = \hat{\mathcal{I}}, \quad (12)$$

where the detailed proof can be found in Eq. (28) of Ref. 51.

The SW transform in Eq. (10) constructs a mapping between an operator in the Hilbert space and a continuous function whose variables are $\{\theta, \varphi\}$ or $\{\Omega\}$ on the $SU(N)$ Lie group/manifold. More specifically, this mapping formalism establishes the following relation:

$$\hat{A} \rightarrow [\hat{A}]_s(\Omega), \quad (13)$$

which is the basic idea of the generalized spin-mapping approach.^{43,44,51}

To conveniently evaluate any operator \hat{A} under the SW transform, one first writes it using the GGM basis, $\{\hat{S}_k\}$, as follows:

$$\hat{A} = \mathcal{A}_0 \cdot \hat{\mathcal{I}} + \frac{1}{\hbar} \sum_{k=1}^{N^2-1} \mathcal{A}_k \cdot \hat{S}_k, \quad (14)$$

where \mathcal{A}_0 and \mathcal{A}_k are expressed as

$$\mathcal{A}_0 = \frac{1}{N} \text{Tr}_e[\hat{A} \cdot \hat{\mathcal{I}}] = \frac{1}{N} \sum_{n=1}^N A_{nn}, \quad (15a)$$

$$\mathcal{A}_k = \frac{2}{\hbar} \text{Tr}_e[\hat{A} \cdot \hat{S}_k], \quad (15b)$$

with the following detailed expressions of \mathcal{A}_k as follows:

$$\mathcal{A}_{\alpha_{nm}} = A_{mn} + A_{nm}, \quad (16a)$$

$$\mathcal{A}_{\beta_{nm}} = i(A_{mn} - A_{nm}), \quad (16b)$$

$$\mathcal{A}_{\gamma_n} = \sum_{l=1}^{n-1} \sqrt{\frac{2}{n(n-1)}} A_{ll} - \sqrt{\frac{2(n-1)}{n}} A_{nn}. \quad (16c)$$

Using the expression of the SW kernel in Eq. (11), the SW transform of \hat{A} is expressed [using Eq. (10)] as

$$[\hat{A}]_s(\Omega) = \mathcal{A}_0 + r_s \sum_{k=1}^{N^2-1} \mathcal{A}_k \cdot \Omega_k. \quad (17)$$

One of the important properties of the SW transform is that it can be used to evaluate a quantum mechanical trace in the continuous phase space as follows:

$$\int d\Omega [\hat{A}]_s(\Omega) = \text{Tr}_e[\hat{A}]. \quad (18)$$

For two operators \hat{A} and \hat{B} , it can be shown that the SW transform has the following property:

$$\begin{aligned} \text{Tr}_e[\hat{A}\hat{B}] &= \int d\Omega [\hat{A}\hat{B}]_s(\Omega) \\ &= \int d\Omega [\hat{A}]_s(\Omega) \cdot [\hat{B}]_s(\Omega) = \int d\Omega [\hat{A}]_s(\Omega) \cdot [\hat{B}]_s(\Omega), \end{aligned} \quad (19)$$

where $[\dots]_s(\Omega)$ is SW transformed through Eq. (17) using r_s instead of r_s . The sum of the squares of the generators [the so-called Casimir operator of $\mathfrak{su}(N)$] requires that⁴⁴

$$r_s \cdot r_{\bar{s}} = N + 1. \quad (20)$$

The commonly used values^{44,48} of r_s and $r_{\bar{s}}$ is the following symmetrical choice:

$$r_s = r_{\bar{s}} = \sqrt{N + 1}. \quad (21)$$

These parameters are not restricted to the above special case, and they can take any value in the range $r_s \in (0, \infty)$. The exact quantum dynamics is invariant under the choice of r_s , but the approximate quantum dynamics methods are not. Previous studies from both the linearized method^{44,51} and the spin mapping NRPMD⁵² suggest that Eq. (21) gives the best numerical performances for computing regular TCF^{44,51} and Kubo-transformed TCF⁵² (for two-level systems).

Another useful relation of the SW transform is

$$\begin{aligned} [\hat{A}\hat{B}]_s(\Omega) &= \mathcal{A}_0\mathcal{B}_0 + \frac{1}{2N} \sum_{i=1}^{N^2-1} \mathcal{A}_i\mathcal{B}_i + r_s \sum_{i=1}^{N^2-1} (\Omega_i\mathcal{A}_i\mathcal{B}_0 + \Omega_i\mathcal{A}_0\mathcal{B}_i) \\ &\quad + \frac{r_s}{2} \sum_{i,j,k=1}^{N^2-1} \Omega_i\mathcal{A}_j\mathcal{B}_k(d_{ijk} + if_{ijk}). \end{aligned} \quad (22)$$

The detailed derivation of this expression can be found in Eqs. (41) and (42) of Ref. 51.

C. The mixed Stratonovich–Weyl/Wigner representation

For the nuclear DOF, one often uses the following Wigner (W) transform:⁶⁷

$$[\hat{O}(\hat{R}, \hat{P})]_w = \int d\Delta e^{\frac{i}{\hbar} P \Delta} \left(R - \frac{\Delta}{2} \right) [\hat{O}(\hat{R}, \hat{P})] \left(R + \frac{\Delta}{2} \right), \quad (23)$$

which converts an operator \hat{O} into a phase space function $[\hat{O}(\hat{R}, \hat{P})]_w$.

For a general operator in the electronic and nuclear Hilbert space, we use the SW representation for the electronic subsystem that exhibits $SU(N)$ symmetry and the Wigner transform for the nuclear DOF. This mixed Stratonovich–Weyl/Wigner (SW/W) formalism was introduced in our previous work to approximately evaluate the regular TCF.⁵¹ For an operator $\hat{A}(\hat{R}, \hat{P})$, the mixed SW/W transform is

$$\begin{aligned} [\hat{A}(\hat{R}, \hat{P})]_{ws} &= [\mathcal{A}_0(\hat{R}, \hat{P})]_w + r_s \sum_{k=1}^{N^2-1} [\mathcal{A}_k(\hat{R}, \hat{P})]_w \cdot \Omega_k \\ &= \mathcal{A}_0(R, P) + r_s \sum_{k=1}^{N^2-1} \mathcal{A}_k(R, P) \cdot \Omega_k, \end{aligned} \quad (24)$$

where $\mathcal{A}_0(R, P)$ and $\mathcal{A}_k(R, P)$ are Wigner transforms of $\mathcal{A}_0(\hat{R}, \hat{P})$ and $\mathcal{A}_k(\hat{R}, \hat{P})$, respectively, with the detailed forms of \mathcal{A}_0 and \mathcal{A}_k defined in Eq. (15).

Furthermore, for two operators, the mixed SW/W representation is expressed as

$$\begin{aligned} [\hat{A}\hat{B}]_{ws} &= \mathcal{A}_0 e^{-i\frac{\hat{A}\hbar}{2}} \mathcal{B}_0 + \frac{1}{2N} \sum_{i=1}^{N^2-1} \mathcal{A}_i e^{-i\frac{\hat{A}\hbar}{2}} \mathcal{B}_i \\ &\quad + r_s \sum_{i=1}^{N^2-1} \Omega_i \left(\mathcal{A}_i e^{-i\frac{\hat{A}\hbar}{2}} \mathcal{B}_0 + \mathcal{A}_0 e^{-i\frac{\hat{A}\hbar}{2}} \mathcal{B}_i \right) \\ &\quad + \frac{r_s}{2} \sum_{i,j,k=1}^{N^2-1} \Omega_i \mathcal{A}_j e^{-i\frac{\hat{A}\hbar}{2}} \mathcal{B}_k (d_{ijk} + if_{ijk}), \end{aligned} \quad (25)$$

where

$$\hat{A} = \frac{\overleftarrow{\partial}}{\partial P} \frac{\overrightarrow{\partial}}{\partial R} - \frac{\overleftarrow{\partial}}{\partial R} \frac{\overrightarrow{\partial}}{\partial P} \quad (26)$$

is the negative Poisson operator associated with the nuclear DOF.^{68–70} Note that for convenience we write \mathcal{A}_0 instead of $\mathcal{A}_0(R, P)$, and the same applies to $\mathcal{A}_i(R, P)$, $\mathcal{B}_0(R, P)$, and $\mathcal{B}_i(R, P)$.

III. THE KUBO-TRANSFORMED TIME-CORRELATION FUNCTION

The Kubo-transformed TCF is defined as follows:

$$\begin{aligned} C_{AB}^K(t) &= \frac{1}{Z\beta} \int_0^\beta d\lambda \text{Tr} \left[e^{-(\beta-\lambda)\hat{H}} \hat{A} e^{-\lambda\hat{H}} e^{\frac{i}{\hbar}\hat{H}t} \hat{B} e^{-\frac{i}{\hbar}\hat{H}t} \right] \\ &= \frac{1}{Z\mathcal{N}} \sum_{\alpha=1}^{\mathcal{N}} \text{Tr} \left[e^{-\beta_N(\mathcal{N}-\alpha)\hat{H}} \hat{A} e^{-\beta_N\alpha\hat{H}} e^{\frac{i}{\hbar}\hat{H}t} \hat{B} e^{-\frac{i}{\hbar}\hat{H}t} \right], \end{aligned} \quad (27)$$

where $\beta = 1/k_B T$, $\beta_N \equiv \beta/\mathcal{N}$, and $\text{Tr}[\dots] \equiv \text{Tr}_n \text{Tr}_e[\dots]$ is a trace over nuclear and electronic DOFs and $Z = \text{Tr}[e^{-\beta\hat{H}}]$. Note that the index α is used to represent a discrete version of the imaginary time integral over λ , not to be confused with α_{nm} , the label of the $\mathfrak{su}(N)$ generators used in Eq. (6). We will later identify that index α as the nuclear bead index. In this section, we use the mixed SW/W representation to re-express $C_{AB}^K(t)$, and derive the exact quantum Liouvillian.

A. The Kubo-transformed TCF in the mixed SW/W representation

To evaluate the Kubo-transformed TCF, we follow the previous strategy^{25,30,71,72} to use the discretized expression in the second line of $C_{AB}^K(t)$ in Eq. (27). We write the Kubo-transformed TCF in a block form by inserting $\mathcal{N}-1$ identities, $\hat{I} = e^{\frac{i}{\hbar}\hat{H}t} e^{-\frac{i}{\hbar}\hat{H}t}$, into Eq. (27), leading to

$$\begin{aligned} C_{AB}^{[\mathcal{N}]}(t) &= \frac{1}{Z\mathcal{N}} \sum_{\alpha=1}^{\mathcal{N}} \text{Tr}_e \text{Tr}_n \left[\left(e^{-\beta_N\hat{H}} e^{\frac{i}{\hbar}\hat{H}t} e^{-\frac{i}{\hbar}\hat{H}t} \right)^{\mathcal{N}-\alpha-1} \right. \\ &\quad \times e^{-\beta_N\hat{H}} \hat{A} e^{\frac{i}{\hbar}\hat{H}t} e^{-\frac{i}{\hbar}\hat{H}t} \left(e^{-\beta_N\hat{H}} e^{\frac{i}{\hbar}\hat{H}t} e^{-\frac{i}{\hbar}\hat{H}t} \right)^{\alpha-1} \\ &\quad \left. \times e^{-\beta_N\hat{H}} e^{\frac{i}{\hbar}\hat{H}t} \hat{B} e^{-\frac{i}{\hbar}\hat{H}t} \right]. \end{aligned} \quad (28)$$

To evaluate the above trace, we insert the nuclear identity $\hat{1}_{R'_1} = \int dR'_1 |R'_1\rangle\langle R'_1| \otimes \hat{\mathcal{I}}$ (where $\hat{\mathcal{I}}$ is the electronic identity) and use the property of the SW transform in Eq. (18) to compute electronic traces, leading to the following expression:

$$\begin{aligned} C_{AB}^{[\mathcal{N}]}(t) &= \frac{1}{Z\mathcal{N}} \sum_{\alpha=1}^{\mathcal{N}} \int dR'_1 \int d\Omega^{(1)} \left[\left\langle R'_1 \middle| e^{\frac{i}{\hbar}\hat{H}t} e^{-\frac{i}{\hbar}\hat{H}t} \right. \right. \\ &\quad \times \left(e^{-\beta_N\hat{H}} e^{\frac{i}{\hbar}\hat{H}t} e^{-\frac{i}{\hbar}\hat{H}t} \right)^{\mathcal{N}-\alpha-2} e^{-\beta_N\hat{H}} \hat{A} e^{\frac{i}{\hbar}\hat{H}t} e^{-\frac{i}{\hbar}\hat{H}t} \\ &\quad \times \left. \left. \left(e^{-\beta_N\hat{H}} e^{\frac{i}{\hbar}\hat{H}t} e^{-\frac{i}{\hbar}\hat{H}t} \right)^{\alpha-1} e^{-\beta_N\hat{H}} e^{\frac{i}{\hbar}\hat{H}t} \hat{B} e^{-\frac{i}{\hbar}\hat{H}t} \right. \right. \\ &\quad \left. \left. \times e^{-\beta_N\hat{H}} \right| R'_1 \right]_s^{(1)}, \end{aligned} \quad (29)$$

where we denote $[\dots]_s^{(\alpha)}$ as the SW transform of the α th coherent state basis $|\Omega^{(\alpha)}\rangle$ as follows:

$$[\hat{A}]_s^{(\alpha)} = \text{Tr}_e [\hat{A} \cdot \hat{w}_s^{(\alpha)}], \quad (30a)$$

$$\hat{w}_s^{(\alpha)} = \frac{1}{N} \hat{\mathcal{I}} + r_s \cdot \frac{2}{\hbar} \sum_{k=1}^{N^2-1} \Omega_k^{(\alpha)} \cdot \hat{\mathcal{S}}_k, \quad (30b)$$

$$\Omega_k^{(\alpha)} \equiv \langle \Omega^{(\alpha)} | \hat{\mathcal{S}}_k | \Omega^{(\alpha)} \rangle. \quad (30c)$$

We then use the following electronic identities [see Eq. (12)] and nuclear identities:

$$\hat{1}_{R'_y, \Omega^{(y)}} = \int dR'_y |R'_y\rangle\langle R'_y| \otimes \int d\Omega^{(y)} \hat{w}_s^{(y)}, \quad (31a)$$

$$\hat{1}_{R''_y} = \int dR''_y |R''_y\rangle\langle R''_y| \otimes \hat{\mathcal{I}}, \quad (31b)$$

where $y = 1, \dots, \mathcal{N}$. The identity $\hat{1}_{R'_y, \Omega^{(y)}}$ is inserted after each $e^{-\beta_N\hat{H}}$ and $\hat{1}_{R''_y}$ is inserted after each $e^{\frac{i}{\hbar}\hat{H}t} e^{-\frac{i}{\hbar}\hat{H}t}$, leading to

$$\begin{aligned} C_{AB}^{[\mathcal{N}]}(t) &= \frac{1}{Z} \int d\{R'_\alpha\} \int d\{R''_\alpha\} \int d\{\Omega^{(\alpha)}\} \\ &\quad \times \frac{1}{\mathcal{N}} \sum_{\alpha=1}^{\mathcal{N}} \left[\left\langle R'_1 \middle| e^{i\hat{H}t/\hbar} e^{-i\hat{H}t/\hbar} \hat{1}_{R''_1} \right. \right. \\ &\quad \times \prod_{y=2}^{\mathcal{N}-\alpha-1} e^{-\beta_N\hat{H}} \hat{1}_{R'_y, \Omega^{(y)}} e^{\frac{i}{\hbar}\hat{H}t} e^{-\frac{i}{\hbar}\hat{H}t} \hat{1}_{R''_y} \\ &\quad \times e^{-\beta_N\hat{H}} \hat{A} \hat{1}_{R'_y, \Omega^{(\mathcal{N}-\alpha)}} e^{\frac{i}{\hbar}\hat{H}t} e^{-\frac{i}{\hbar}\hat{H}t} \hat{1}_{R''_{\mathcal{N}-\alpha}} \\ &\quad \times \prod_{y=\mathcal{N}-\alpha+1}^{\mathcal{N}-1} e^{-\beta_N\hat{H}} \hat{1}_{R'_y, \Omega^{(y)}} e^{\frac{i}{\hbar}\hat{H}t} e^{-\frac{i}{\hbar}\hat{H}t} \hat{1}_{R''_y} \\ &\quad \left. \left. \times e^{-\beta_N\hat{H}} \hat{1}_{R'_{\mathcal{N}}, \Omega^{(\mathcal{N})}} e^{\frac{i}{\hbar}\hat{H}t} \hat{B} e^{-\frac{i}{\hbar}\hat{H}t} \hat{1}_{R''_{\mathcal{N}}} e^{-\beta_N\hat{H}} \right| R'_1 \right]_s^{(1)}, \end{aligned} \quad (32)$$

where we have introduced the shorthand notation $d\{R'_\alpha\} \equiv \prod_{\alpha=1}^{\mathcal{N}} dR'_\alpha$, $d\{R''_\alpha\} \equiv \prod_{\alpha=1}^{\mathcal{N}} dR''_\alpha$, and $d\{\Omega^{(\alpha)}\} \equiv \prod_{\alpha=1}^{\mathcal{N}} d\Omega^{(\alpha)}$, with each $d\Omega^{(\alpha)}$ expressed in Eq. (B2).

Using the properties of the SW transform [Eqs. (10) and (18)], we can rewrite Eq. (32) as follows:

$$\begin{aligned} C_{AB}^{[\mathcal{N}]}(t) &= \frac{1}{Z} \int d\{R'_\alpha\} \int d\{R''_\alpha\} \int d\{\Omega^{(\alpha)}\} \frac{1}{\mathcal{N}} \sum_{\alpha=1}^{\mathcal{N}} \text{Tr}_e \\ &\quad \times \left[\prod_{y \neq \alpha}^{\mathcal{N}} \left\langle R''_{y-1} \middle| e^{-\beta_N\hat{H}} \right| R'_y \right] \hat{w}_s^{(y)} \left\langle R''_{\alpha-1} \middle| e^{-\beta_N\hat{H}} \hat{A} \right| R'_\alpha \hat{w}_s^{(\alpha)} \Bigg] \\ &\quad \times \frac{1}{\mathcal{N}} \sum_{\alpha=1}^{\mathcal{N}} \sum_{y \neq \alpha}^{\mathcal{N}} \left[\left\langle R''_y \middle| e^{\frac{i}{\hbar}\hat{H}t} e^{-\frac{i}{\hbar}\hat{H}t} \right| R'_y \right]_s^{(y)} \\ &\quad \times \left[\left\langle R''_\alpha \middle| e^{\frac{i}{\hbar}\hat{H}t} \hat{B} e^{-\frac{i}{\hbar}\hat{H}t} \right| R'_\alpha \right]_s^{(\alpha)}, \end{aligned} \quad (33)$$

where we have used the cyclic-symmetric property to write the operator \hat{B} into a bead-averaged fashion (index α can be viewed as a bead index of a ring-polymer of \mathcal{N} beads). Note that the two sums with respect to α are two independent ones. The details of the derivation are provided in Appendix C.

We can now change the nuclear variables^{71,72} as the following mean and difference variables:

$$R_\alpha = \frac{1}{2} (R'_\alpha + R''_\alpha), \quad (34a)$$

$$D_\alpha = R'_\alpha - R''_\alpha \quad (34b)$$

and insert the following identity for each block:

$$1 = \int dD'_\alpha \delta(D_\alpha + D'_\alpha) = \frac{1}{2\pi\hbar} \int dD'_\alpha \int dP_\alpha e^{\frac{i}{\hbar}P_\alpha(D_\alpha + D'_\alpha)}. \quad (35)$$

This leads to the Wigner representation of the nuclear DOFs, and the TCF in Eq. (33) becomes

$$C_{AB}^{[\mathcal{N}]}(t) = \frac{1}{\mathcal{Z}(2\pi\hbar)^{\mathcal{N}}} \int d\{R_\alpha\} \int d\{P_\alpha\} \int d\{\Omega^{(\alpha)}\} \times [e^{-\beta\hat{H}} \hat{A}]_{ws} [\hat{B}(t)]_{ws}, \quad (36)$$

where $[e^{-\beta\hat{H}} \hat{A}]_{ws}$ is the SW/W transformed Boltzmann operator expressed as

$$[e^{-\beta\hat{H}} \hat{A}]_{ws} = \int d\{D_\alpha\} \frac{1}{\mathcal{N}} \sum_{\alpha=1}^{\mathcal{N}} \prod_{\gamma=1}^{\mathcal{N}} e^{iP_\gamma D_\gamma/\hbar} \times \text{Tr}_e \left[\prod_{\gamma \neq \alpha}^{\mathcal{N}} \left(R_{\gamma-1} - \frac{1}{2} D_{\gamma-1} \right| e^{-\beta\mathcal{N}\hat{H}} \left| R_\gamma + \frac{1}{2} D_\gamma \right) \hat{w}_s^{(\gamma)} \right] \times \left(R_{\alpha-1} - \frac{1}{2} D_{\alpha-1} \right| e^{-\beta\mathcal{N}\hat{H}} \hat{A} \left| R_\alpha + \frac{1}{2} D_\alpha \right) \hat{w}_s^{(\alpha)} \quad (37)$$

and $[\hat{B}(t)]_{ws}$ is the bead-averaged SW/W transform of operator \hat{B} expressed as follows:

$$[\hat{B}(t)]_{ws} = \int d\{D'_\alpha\} \frac{1}{\mathcal{N}} \sum_{\alpha=1}^{\mathcal{N}} \prod_{\gamma=1}^{\mathcal{N}} e^{iP_\gamma D'_\gamma/\hbar} \times \prod_{\gamma \neq \alpha}^{\mathcal{N}} \left[\left(R_\gamma - \frac{1}{2} D'_\gamma \right| e^{\frac{i}{\hbar}\hat{H}t} e^{-\frac{i}{\hbar}\hat{H}t} \left| R_\gamma + \frac{1}{2} D'_\gamma \right) \right]^{(\gamma)} \times \left[\left(R_\alpha - \frac{1}{2} D'_\alpha \right| e^{\frac{i}{\hbar}\hat{H}t} \hat{B} e^{-\frac{i}{\hbar}\hat{H}t} \left| R_\alpha + \frac{1}{2} D'_\alpha \right) \right]^{(\alpha)} = \frac{1}{\mathcal{N}} \sum_{\alpha=1}^{\mathcal{N}} [\hat{B}(t)]_{ws}^{(\alpha)}. \quad (38)$$

Note that we use the notation $[\hat{B}(t)]_{ws}$ to represent the bead averaged SW/W transform. When introduced in Eq. (25), it was only for a single bead.

We can formally express the Kubo-transformed TCF in Eq. (36) as follows:

$$C_{AB}^{[\mathcal{N}]}(t) = \frac{1}{\mathcal{Z}(2\pi\hbar)^{\mathcal{N}}} \int d\{R_\alpha\} \int d\{P_\alpha\} \int d\{\Omega^{(\alpha)}\} \times [e^{-\beta\hat{H}} \hat{A}]_{ws} e^{\mathcal{L}t} [\hat{B}]_{ws}, \quad (39)$$

where the time-evolution is governed by the quantum Liouvillian,

$$[\hat{B}(t)]_{ws} = e^{\mathcal{L}t} [\hat{B}]_{ws}, \quad (40)$$

which will be derived in Sec. III B.

If, in addition, \hat{A} is linear in \hat{R} (and equivalently for \hat{P}), then

$$[e^{-\beta\hat{H}} \hat{A}]_{ws} = [\hat{A}]_w [e^{-\beta\hat{H}}]_{ws} = \mathcal{A}_0(R) [e^{-\beta\hat{H}}]_{ws}, \quad (41)$$

where we have used $[\hat{A}(\hat{R})]_{ws} = [\mathcal{A}_0(\hat{R})]_w = \mathcal{A}_0(R)$. Due to the cyclic property of the beads, the estimator $\mathcal{A}_0(R)$ is expressed as a bead-average $\mathcal{A}_0(R) \equiv \frac{1}{\mathcal{N}} \sum_{\alpha=1}^{\mathcal{N}} \mathcal{A}_0(R_\alpha)$. In this case, the Kubo-transformed TCF is

$$C_{AB}^{[\mathcal{N}]}(t) = \frac{1}{\mathcal{Z}(2\pi\hbar)^{\mathcal{N}}} \int d\{R_\alpha\} \int d\{P_\alpha\} \int d\{\Omega^{(\alpha)}\} \times \mathcal{A}_0(R) [e^{-\beta\hat{H}}]_{ws} e^{\mathcal{L}t} [\hat{B}]_{ws}. \quad (42)$$

The estimator $[\hat{B}]_{ws}$ [in Eq. (38)] can be expressed [using Eq. (24)] as

$$[\hat{B}]_{ws} = \frac{1}{\mathcal{N}} \sum_{\alpha=1}^{\mathcal{N}} [\hat{B}]_{ws}^{(\alpha)} \times \frac{1}{\mathcal{N}} \sum_{\alpha=1}^{\mathcal{N}} \left(\mathcal{B}_0^{(\alpha)} + r_s \sum_{k=1}^{N^2-1} \mathcal{B}_k^{(\alpha)} \cdot \Omega_k^{(\alpha)} \right), \quad (43)$$

with the short notation $[\hat{B}]_{ws}^{(\alpha)} \equiv [\hat{B}(\hat{R}_\alpha, \hat{P}_\alpha)]_{ws}$, $\mathcal{B}_0^{(\alpha)} \equiv \mathcal{B}_0(R_\alpha, P_\alpha)$, and $\mathcal{B}_k^{(\alpha)} \equiv \mathcal{B}_k(R_\alpha, P_\alpha)$. This expression is a bead average of the mixed SW/W transform of the operator \hat{B} . If it is a position operator, $\hat{B} = \hat{R}$,

$$[\hat{B}]_{ws} = \frac{1}{\mathcal{N}} \sum_{\alpha=1}^{\mathcal{N}} [\hat{R}_\alpha]_w = \frac{1}{\mathcal{N}} \sum_{\alpha=1}^{\mathcal{N}} R_\alpha. \quad (44)$$

If \hat{B} is a projection operator $\hat{B} = |n\rangle\langle m|$, then the corresponding expression becomes

$$[\hat{B}]_{ws} = \frac{1}{\mathcal{N}} \sum_{\alpha=1}^{\mathcal{N}} [|n\rangle\langle m|]_s^{(\alpha)}. \quad (45)$$

This projection operator can be expressed in terms of different mapping variables, which can be found in our previous work [Eqs. (44) and (45), (62)–(64), and (D8)–(D10) in Ref. 51]. In terms of the spin mapping variables $\{\Omega_k^{(\alpha)}\}$ in Eq. (9) (for $n > m$), we have

$$[|n\rangle\langle n|]_s^{(\alpha)} = \frac{1}{N} + r_s \sum_{m=n+1}^N \sqrt{\frac{2}{m(m-1)}} \Omega_{\gamma_m}^{(\alpha)} - r_s \sqrt{\frac{2(n-1)}{n}} \Omega_{\gamma_n}^{(\alpha)}, \quad (46a)$$

$$[|n\rangle\langle m|]_s^{(\alpha)} = r_s \left(\Omega_{\alpha nm}^{(\alpha)} - i\Omega_{\beta nm}^{(\alpha)} \right), \quad (46b)$$

$$[|m\rangle\langle n|]_s^{(\alpha)} = r_s \left(\Omega_{\alpha nm}^{(\alpha)} + i\Omega_{\beta nm}^{(\alpha)} \right), \quad (46c)$$

where the detailed expressions of $\Omega_{\alpha nm}$, $\Omega_{\beta nm}$, and Ω_{γ_m} are provided in Eqs. (B5)–(B7).

B. Expression of the quantum Liouvillian

To obtain the quantum Liouvillian \mathcal{L} [in Eq. (40)], we use the time-derivative of $[\hat{B}]_{ws}$ through the Heisenberg equations of motions (EOMs) as follows:

$$\frac{d}{dt} [\hat{B}]_{ws} = \mathcal{L} [\hat{B}]_{ws} = \frac{1}{\mathcal{N}} \sum_{\alpha=1}^{\mathcal{N}} \frac{d}{dt} [\hat{B}]_{ws}^{(\alpha)} = \frac{1}{\mathcal{N}} \sum_{\alpha=1}^{\mathcal{N}} \mathcal{L}^{(\alpha)} [\hat{B}]_{ws}^{(\alpha)}, \quad (47)$$

leading to an expression of bead specific Liouvillian components, $\mathcal{L}^{(\alpha)}$, evolving each bead. Each of these Liouvillian components is identical to what we have previously derived for a regular TCF.⁵¹ The expression of $\mathcal{L}^{(\alpha)}$ is obtained through

$$\begin{aligned} \frac{d}{dt} [\hat{B}]_{ws}^{(\alpha)} &= \frac{d}{dt} [\mathcal{B}_0 \hat{\mathcal{I}}]_{ws}^{(\alpha)} + \sum_{i=1}^{N^2-1} \frac{d}{dt} \left[\mathcal{B}_i \cdot \frac{1}{\hbar} \hat{\mathcal{S}}_i \right]_{ws}^{(\alpha)} \\ &= \frac{d}{dt} [\mathcal{B}_0]_w^{(\alpha)} + \sum_{i=1}^{N^2-1} \frac{d}{dt} \left([\mathcal{B}_i]_w^{(\alpha)} \cdot r_s \Omega_i^{(\alpha)} \right) \\ &\equiv \mathcal{L}_0^{(\alpha)} \mathcal{B}_0^{(\alpha)} + r_s \sum_{i=1}^{N^2-1} \mathcal{L}_i^{(\alpha)} \left(\Omega_i^{(\alpha)} \mathcal{B}_i^{(\alpha)} \right). \end{aligned} \quad (48)$$

The state-independent Liouvillian $\mathcal{L}_0^{(\alpha)}$ is expressed as

$$\mathcal{L}_0^{(\alpha)} \mathcal{B}_0^{(\alpha)} \equiv \frac{2}{\hbar} H_s(R_\alpha, P_\alpha) \sin\left(\frac{\hbar}{2} \hat{\Lambda}_\alpha\right) \mathcal{B}_0^{(\alpha)}, \quad (49)$$

with the SW/W transform of the Hamiltonian

$$\begin{aligned} H_s(R_\alpha, P_\alpha) &\equiv [\hat{H}(\hat{R}_\alpha, \hat{P}_\alpha)]_{ws} \\ &= \mathcal{H}_0(R_\alpha, P_\alpha) + r_s \sum_{k=1}^{N^2-1} \mathcal{H}_k(R_\alpha) \Omega_k^{(\alpha)}, \end{aligned} \quad (50a)$$

$$\mathcal{H}_0(R_\alpha, P_\alpha) = \frac{P_\alpha^2}{2m} + U_0(R_\alpha) + \frac{1}{N} \sum_{n=1}^N V_{nn}(R_\alpha), \quad (50b)$$

$$\mathcal{H}_k(R_\alpha) = \frac{2}{\hbar} \text{Tr}_e [\hat{V}_e(R_\alpha) \cdot \hat{\mathcal{S}}_k], \quad (50c)$$

and the negative Poisson operator for the α_{th} bead is

$$\hat{\Lambda}_\alpha = \frac{\overleftarrow{\partial}}{\partial P_\alpha} \frac{\overrightarrow{\partial}}{\partial R_\alpha} - \frac{\overleftarrow{\partial}}{\partial R_\alpha} \frac{\overrightarrow{\partial}}{\partial P_\alpha}. \quad (51)$$

The state-dependent Liouvillian is split into two terms, $\mathcal{L}_i^{(\alpha)} = \mathcal{L}_i^{e(\alpha)} + \mathcal{L}_i^{n(\alpha)}$. The first term $\mathcal{L}_i^{e(\alpha)}$ evolves the spin mapping variables (electronic DOFs) as

$$\mathcal{L}_i^{e(\alpha)} \left(r_s \Omega_i^{(\alpha)} \mathcal{B}_i^{(\alpha)} \right) \equiv \frac{r_s}{\hbar} \sum_{j,k=1}^{N^2-1} f_{ijk} \mathcal{H}_j(R_\alpha) \Omega_k^{(\alpha)} \cos\left(\frac{\hbar}{2} \hat{\Lambda}_\alpha\right) \mathcal{B}_i^{(\alpha)}, \quad (52)$$

and the second term $\mathcal{L}_i^{n(\alpha)}$ evolves the nuclear DOFs and couples the spin-mapping variables and the nuclear DOFs as follows:

$$\begin{aligned} \mathcal{L}_i^{n(\alpha)} \left(r_s \Omega_i^{(\alpha)} \mathcal{B}_i^{(\alpha)} \right) &\equiv \frac{1}{\hbar} \left[\frac{1}{N} \mathcal{H}_i(R_\alpha) + 2r_s \Omega_i^{(\alpha)} \mathcal{H}_0(R_\alpha, P_\alpha) \right. \\ &\quad \left. + r_s \sum_{j,k=1}^{N^2-1} d_{ijk} \mathcal{H}_j(R_\alpha) \Omega_k^{(\alpha)} \right] \sin\left(\frac{\hbar}{2} \hat{\Lambda}_\alpha\right) \mathcal{B}_i^{(\alpha)}, \end{aligned} \quad (53)$$

and note that the $1/N$ in Eq. (53) comes from the SW transform (where N is the number of electronic states, not to be confused with the total number of beads \mathcal{N}).

These Liouvillian expressions give rise to the time evolution of each bead, α , as follows:

$$\begin{aligned} \mathcal{L}[\hat{B}]_{ws} &= \frac{1}{\mathcal{N}} \sum_{\alpha=1}^{\mathcal{N}} \mathcal{L}^{(\alpha)} [\hat{B}]_{ws}^{(\alpha)} \\ &= \frac{1}{\mathcal{N}} \sum_{\alpha=1}^{\mathcal{N}} \left[\mathcal{L}_0^{(\alpha)} \mathcal{B}_0^{(\alpha)} + r_s \sum_{i=1}^{N^2-1} (\mathcal{L}_i^{e(\alpha)} + \mathcal{L}_i^{n(\alpha)}) \Omega_i^{(\alpha)} \mathcal{B}_i^{(\alpha)} \right]. \end{aligned} \quad (54)$$

We emphasize that the Kubo-transformed TCF in Eq. (39) and the Liouvillian in Eq. (54) are, in principle, exact. Directly evaluating these expressions numerically will be as difficult as the exact quantum mechanics.

IV. NON-ADIABATIC MATSUBARA DYNAMICS AND SM-NRPMD

In this section, we follow the original work on the Matsubara dynamics in Ref. 30 as well as our recent work on non-adiabatic Matsubara dynamics based on the MMST mapping variables to derive the spin mapping based non-adiabatic Matsubara and the spin-mapping non-adiabatic RPMD (SM-NRPMD) approach.

A. Non-adiabatic Matsubara dynamics

We follow the procedure of our previous work²⁵ on deriving the non-adiabatic Matsubara dynamics. First, a transformation from the bead to the normal mode representation is introduced as follows:

$$\mathcal{R}_l = \sum_{\alpha=1}^{\mathcal{N}} \frac{T_{\alpha l}}{\sqrt{\mathcal{N}}} R_\alpha, \quad \mathcal{P}_l = \sum_{\alpha=1}^{\mathcal{N}} \frac{T_{\alpha l}}{\sqrt{\mathcal{N}}} P_\alpha, \quad (55)$$

and the corresponding inverse transform is

$$R_\alpha = \sum_{l=-\frac{\mathcal{N}-1}{2}}^{\frac{\mathcal{N}-1}{2}} T_{\alpha l} \sqrt{\mathcal{N}} \mathcal{R}_l, \quad P_\alpha = \sum_{l=-\frac{\mathcal{N}-1}{2}}^{\frac{\mathcal{N}-1}{2}} T_{\alpha l} \sqrt{\mathcal{N}} \mathcal{P}_l, \quad (56)$$

with the transformation matrix element (with an odd number \mathcal{N}) defined as

$$T_{\alpha l} = \begin{cases} \sqrt{\frac{1}{\mathcal{N}}}, & l = 0, \\ \sqrt{\frac{2}{\mathcal{N}}} \sin \frac{2\pi\alpha l}{\mathcal{N}}, & 1 \leq l \leq \frac{\mathcal{N}-1}{2}, \\ \sqrt{\frac{2}{\mathcal{N}}} \cos \frac{2\pi\alpha l}{\mathcal{N}}, & -\frac{\mathcal{N}-1}{2} \leq l \leq -1. \end{cases} \quad (57)$$

The new variables $\{\mathcal{R}_l, \mathcal{P}_l\}$ are normal modes of the free ring polymer Hamiltonian

$$\begin{aligned} \mathcal{H}_{rp}^0 &= \sum_{\alpha=1}^{\mathcal{N}} \left[\frac{P_\alpha^2}{2m} + \frac{m}{2\beta_N^2 \hbar^2} (R_\alpha - R_{\alpha-1})^2 \right] \\ &= \mathcal{N} \sum_{l=-\frac{\mathcal{N}-1}{2}}^{\frac{\mathcal{N}-1}{2}} \frac{\mathcal{P}_l^2}{2m} + \frac{m}{2} \omega_l^2 \mathcal{R}_l^2, \end{aligned} \quad (58)$$

where the normal mode frequency is

$$\omega_l = \frac{2}{\beta_N \hbar} \sin\left(\frac{l\pi}{\mathcal{N}}\right), \quad (59)$$

and $l = 0, \dots, \pm(\mathcal{N} - 1)/2$ is the index of normal modes. Using this transformation, the Liouvillian in Eqs. (49)–(53) can be expressed in the normal mode representation using the Poisson operator expressed in terms of the normal modes. The estimator $[\hat{B}]_{\text{ws}}^{(\alpha)}$ is also expressed in terms of the normal modes through Eq. (56) as $\mathcal{B}_0^{(\alpha)} \equiv \mathcal{B}_0(R_\alpha(\mathcal{R}), P_\alpha(\mathcal{P}))$ and, equivalently, for $\mathcal{B}_i^{(\alpha)}$.

To transform the bead-specific Liouvillian into normal mode representation, we first write the Poisson operator $\frac{\hbar}{2}\hat{\Lambda}_\alpha$ inside the sines and cosines of Eqs. (49)–(53) as a sum over *all bead indices* $\sum_\alpha \frac{\hbar}{2}\hat{\Lambda}_\alpha$, leading to the following replacement:

$$\begin{aligned} \sin\left(\frac{\hbar}{2}\hat{\Lambda}_\alpha\right) &\rightarrow \sin\left(\frac{\hbar}{2}\sum_{\alpha=1}^{\mathcal{N}}\hat{\Lambda}_\alpha\right), \\ \cos\left(\frac{\hbar}{2}\hat{\Lambda}_\alpha\right) &\rightarrow \cos\left(\frac{\hbar}{2}\sum_{\alpha=1}^{\mathcal{N}}\hat{\Lambda}_\alpha\right). \end{aligned}$$

This results in an identical Liouvillian compared to the original expression^{30,74} because there is no cross-bead term in $H_s(R_\alpha, P_\alpha)$ nor in $\mathcal{H}_j(R_\alpha)$, $\mathcal{B}_0^{(\alpha)}$, and $\mathcal{B}_k^{(\alpha)}$. With these expressions, the Liouvillian can be transformed into the normal mode representation³⁰ as follows:

$$\mathcal{L}_0^{(\alpha)}\mathcal{B}_0^{(\alpha)} = \frac{2}{\hbar}H_s(R_\alpha(\mathcal{R}), P_\alpha(\mathcal{P}))\sin\left(\frac{\hbar}{2\mathcal{N}}\hat{\Lambda}^{[\mathcal{N}]}\right)\mathcal{B}_0^{(\alpha)}, \quad (60\text{a})$$

$$\begin{aligned} \mathcal{L}_i^{e(\alpha)}\left(r_s\Omega_i^{(\alpha)}\mathcal{B}_i^{(\alpha)}\right) &= \frac{r_s}{\hbar}\sum_{j,k=1}^{N^2-1}f_{ijk}\mathcal{H}_j(R_\alpha(\mathcal{R}))\Omega_k^{(\alpha)} \\ &\times \cos\left(\frac{\hbar}{2\mathcal{N}}\hat{\Lambda}^{[\mathcal{N}]}\right)\mathcal{B}_i^{(\alpha)}, \end{aligned} \quad (60\text{b})$$

$$\begin{aligned} \mathcal{L}_i^{n(\alpha)}\left(r_s\Omega_i^{(\alpha)}\mathcal{B}_i^{(\alpha)}\right) &= \left[\frac{1}{N}\mathcal{H}_i(R_\alpha(\mathcal{R})) + 2r_s\Omega_i^{(\alpha)}\mathcal{H}_0(R_\alpha(\mathcal{R}), P_\alpha(\mathcal{P})) \right. \\ &+ r_s\sum_{j,k=1}^{N^2-1}d_{ijk}\mathcal{H}_j(R_\alpha(\mathcal{R}))\Omega_k^{(\alpha)} \\ &\times \sin\left(\frac{\hbar}{2\mathcal{N}}\hat{\Lambda}^{[\mathcal{N}]}\right)\mathcal{B}_i^{(\alpha)}, \end{aligned} \quad (60\text{c})$$

where $\hat{\Lambda}^{[\mathcal{N}]}$ is the Poisson operator with the normal mode representation expressed as follows:

$$\hat{\Lambda}^{[\mathcal{N}]} = \sum_{l=-\frac{\mathcal{N}-1}{2}}^{\frac{\mathcal{N}-1}{2}}\frac{\overleftarrow{\partial}}{\partial\mathcal{P}_l}\frac{\overrightarrow{\partial}}{\partial\mathcal{R}_l} - \frac{\overleftarrow{\partial}}{\partial\mathcal{R}_l}\frac{\overrightarrow{\partial}}{\partial\mathcal{P}_l}. \quad (61)$$

The correlation function in Eq. (39) can be expressed in the normal mode representation as follows:

$$\begin{aligned} C_{AB}^{[\mathcal{N}]}(t) &= \frac{1}{Z(2\pi\hbar)^{\mathcal{N}}}\int d\{\mathcal{R}_l\}\int d\{\mathcal{P}_l\}\int d\{\Omega^{(\alpha)}\} \\ &\times [e^{-\beta\hat{H}}\hat{A}]_{\text{ws}} e^{\mathcal{L}t}[\hat{B}]_{\text{ws}}, \end{aligned} \quad (62)$$

where $d\{\mathcal{R}_l\} \equiv \prod_{l=-(\mathcal{N}-1)/2}^{(\mathcal{N}-1)/2}d\mathcal{R}_l$, $d\{\mathcal{P}_l\} \equiv \prod_{l=-(\mathcal{N}-1)/2}^{(\mathcal{N}-1)/2}d\mathcal{P}_l$, both $[e^{-\beta\hat{H}}\hat{A}]_{\text{ws}}$ and $[\hat{B}]_{\text{ws}}$ are expressed in the normal mode represen-

tation, and the Liouvillian \mathcal{L} is expressed using the normal modes, with the detailed expressions in Eq. (60).

In the limit of $\mathcal{N} \rightarrow \infty$, only the \mathcal{M} lowest frequencies of the free ring-polymer of \mathcal{N} beads (when $\mathcal{M} \ll \mathcal{N}$) contribute to the initial quantum Boltzmann distribution.^{75–77} The frequencies of these modes are referred to as the Matsubara frequencies,^{30,78}

$$\tilde{\omega}_l = \frac{2l\pi}{\beta\hbar}, \quad |l| \leq (\mathcal{M} - 1)/2, \quad (63)$$

which corresponds to the $\mathcal{M} \ll \mathcal{N}$ limit (under the $\mathcal{M} \rightarrow \infty$ and $\mathcal{N} \rightarrow \infty$ limits) of the normal mode frequencies in Eq. (59).

The main idea of the Matsubara dynamics³⁰ is to *only use the Matsubara modes* to evolve the quantum dynamics in the Kubo-transformed TCF because these modes completely determine the initial quantum statistics. Hence, the central approximation of the Matsubara dynamics is to *discard the non-Matsubara modes* in the quantum Liouvillian.³⁰ To briefly discuss this, we introduce the following mode-to-bead transformation that only considering the Matsubara modes:

$$R_\alpha^{[\mathcal{M}]} \equiv R_\alpha(\mathcal{R}_{\mathcal{M}}) = \sum_{l=-\frac{\mathcal{M}-1}{2}}^{\frac{\mathcal{M}-1}{2}}\frac{T_{al}}{\sqrt{\mathcal{N}}}\mathcal{R}_l, \quad (64\text{a})$$

$$P_\alpha^{[\mathcal{M}]} \equiv P_\alpha(\mathcal{P}_{\mathcal{M}}) = \sum_{l=-\frac{\mathcal{M}-1}{2}}^{\frac{\mathcal{M}-1}{2}}T_{al}\sqrt{\mathcal{N}}\mathcal{P}_l, \quad (64\text{b})$$

which have the same expression as those in Eq. (56), except a truncation to the normal modes only including the Matsubara modes. In the above equation, we introduced the notation $\mathcal{R}_{\mathcal{M}} = \{\mathcal{R}_{-\frac{\mathcal{M}-1}{2}}, \dots, \mathcal{R}_{\frac{\mathcal{M}-1}{2}}\}$ and $\mathcal{P}_{\mathcal{M}} = \{\mathcal{P}_{-\frac{\mathcal{M}-1}{2}}, \dots, \mathcal{P}_{\frac{\mathcal{M}-1}{2}}\}$ which are the Matsubara modes.

Following the Matsubara approximation,³⁰ we approximate the Liouvillian in Eq. (48) by only considering the Matsubara modes, leading to

$$\mathcal{L}(\hat{\Lambda}^{[\mathcal{N}]}) \approx \mathcal{L}^{[\mathcal{M}]}(\hat{\Lambda}^{[\mathcal{M}]}) , \quad (65)$$

where we have discarded all non-Matsubara modes. The corresponding approximate Liouvillian has the same formal expression as the one given in Eq. (60), except by replacing $\hat{\Lambda}^{[\mathcal{N}]}$ with $\hat{\Lambda}^{[\mathcal{M}]}$ as follows:

$$\hat{\Lambda}^{[\mathcal{N}]} \rightarrow \hat{\Lambda}^{[\mathcal{M}]} = \sum_{l=-\frac{\mathcal{M}-1}{2}}^{\frac{\mathcal{M}-1}{2}}\frac{\overleftarrow{\partial}}{\partial\mathcal{P}_l}\frac{\overrightarrow{\partial}}{\partial\mathcal{R}_l} - \frac{\overleftarrow{\partial}}{\partial\mathcal{R}_l}\frac{\overrightarrow{\partial}}{\partial\mathcal{P}_l}. \quad (66)$$

One can further expand the sines and cosines in the Liouvillian expression $\mathcal{L}^{[\mathcal{M}]}$, leading to^{25,74}

$$\sin\left(\frac{\hbar}{2\mathcal{N}}\hat{\Lambda}^{[\mathcal{M}]}\right) = \frac{\hbar}{2\mathcal{N}}\hat{\Lambda}^{[\mathcal{M}]} + \mathcal{O}\left(\frac{\mathcal{M}^3\hbar^3}{\mathcal{N}^3}\right), \quad (67\text{a})$$

$$\cos\left(\frac{\hbar}{2\mathcal{N}}\hat{\Lambda}^{[\mathcal{M}]}\right) = 1 + \mathcal{O}\left(\frac{\mathcal{M}^2\hbar^2}{\mathcal{N}^2}\right). \quad (67\text{b})$$

Under the limit $\mathcal{M} \ll \mathcal{N}$, the Planck constant is effectively scaled as $\hbar \rightarrow \hbar\mathcal{M}/\mathcal{N}$ [note the overall scaling of $\mathcal{O}(\hat{\Lambda}^{[\mathcal{M}]}) \sim \mathcal{M}$ due to the

sum in Eq. (66)]. This means that inside the Matsubara subspace, one can effectively scale the Planck constant as small as one desires such that the linearization of the sines and cosines becomes *exact* (but remains an approximation in the full normal mode space).³⁰ The Matsubara Liouvillian $\mathcal{L}^{[\mathcal{M}]}(\hat{A}^{[\mathcal{M}]})$ will only update the Matsubara modes in $\mathcal{B}_0^{(\alpha)}$ and $\mathcal{B}_i^{(\alpha)}$ in Eq. (47) and will no longer evolve the non-Matsubara modes. Eventually, one can analytically integrate out all non-Matsubara modes³⁰ in the Kubo-transformed TCF expression (including those inside $[e^{-\beta\hat{H}}\hat{A}]_{ws}$ as well as inside $[\hat{B}]_{ws}$), as shown in Appendix B of Ref. 25 as well as in Ref. 30.

Using the argument in Eq. (67), i.e., only the leading order of the quantum Liouvillian in the Matsubara space is needed, the Liouvillian in Eq. (65) can be expressed as

$$\begin{aligned} \mathcal{L}^{[\mathcal{M}]}[\hat{B}]_{ws}^{[\mathcal{M}]} &\equiv \frac{1}{N} \sum_{\alpha=1}^N \sum_{l=-\frac{\mathcal{M}-1}{2}}^{\frac{\mathcal{M}-1}{2}} \left[\frac{\mathcal{P}_l}{m} \frac{\partial}{\partial \mathcal{R}_l} - \frac{1}{N} \left[\frac{\partial \mathcal{H}_0(R_\alpha^{[\mathcal{M}]})}{\partial \mathcal{R}_l} \right. \right. \\ &\quad \left. + r_s \sum_{j=1}^{N^2-1} \frac{\partial \mathcal{H}_j(R_\alpha^{[\mathcal{M}]})}{\partial \mathcal{R}_l} \Omega_j^{(\alpha)} \right] \frac{\partial}{\partial \mathcal{P}_l} \Bigg] \mathcal{B}_0^{(\alpha)[\mathcal{M}]} \\ &\quad + \frac{1}{N} \sum_{\alpha=1}^N \sum_{i=1}^{N^2-1} \left[\frac{r_s}{\hbar} \sum_{j,k=1}^{N^2-1} f_{ijk} \mathcal{H}_j(R_\alpha^{[\mathcal{M}]}) \Omega_k^{(\alpha)} \right] \mathcal{B}_i^{(\alpha)[\mathcal{M}]}, \end{aligned} \quad (68)$$

where the SW/W transform of the operator \hat{B} will only contain the Matsubara modes,

$$\mathcal{B}_0^{(\alpha)[\mathcal{M}]} \equiv \mathcal{B}_0(R_\alpha^{[\mathcal{M}]}, P_\alpha^{[\mathcal{M}]}) ; \quad \mathcal{B}_i^{(\alpha)[\mathcal{M}]} \equiv \mathcal{B}_i(R_\alpha^{[\mathcal{M}]}, P_\alpha^{[\mathcal{M}]}) . \quad (69)$$

Note that in the Matsubara Liouvillian [Eq. (68)], we have also ignored the $\mathcal{L}_i^{n(\alpha)}(r_s \Omega_i^{(\alpha)} \mathcal{B}_i^{(\alpha)})$ term [Eq. (60c)]. In the linearized spin-mapping approach, this is an additional Liouvillian that is less straightforward to evaluate using independent trajectory method and has been ignored.^{44,51} This should be viewed as an independent approximation, and the consequences of making this approximation are subjects to future investigations.

Following the same procedure outlined in our early work in Ref. 25, we analytically integrate out the non-Matsubara modes (see Appendix B of Ref. 25) in the Kubo-transformed correlation function. A symmetric Trotter expansion (which is exact under the $N \rightarrow \infty$ limit) is further used to split the Boltzmann operator into a state-dependent and a state-independent term to simplify the distribution expression [see Eq. (B4) in Appendix B of Ref. 25]. Finally, we obtain the Matsubara dynamics expression of the Kubo-transformed TCF. When the operator \hat{A} is a linear nuclear operator, the TCF in Eq. (62) has the final form of

$$\begin{aligned} C_{AB}^{[\mathcal{M}]} &= \frac{\alpha_M}{(2\pi\hbar)^N Z_M} \int d\mathcal{R}_M \int d\mathcal{P}_M \int d\{\Omega^{(\alpha)}\} e^{-\beta_N(H_M - iN\phi_M)} \\ &\quad \times \mathcal{A}_0(\mathcal{R}_M) \text{Tr}_e[\hat{\Gamma}_{\tilde{s}}^{[\mathcal{M}]}] e^{\mathcal{L}^{[\mathcal{M}]}_t} [\hat{B}]_{ws}^{[\mathcal{M}]}, \end{aligned} \quad (70)$$

where $\alpha_M = \frac{\hbar^{1-M}}{(M-1)/2!^2}$, with the shorthand notation $d\mathcal{R}_M \equiv \prod_{l=-(M-1)/2}^{(M-1)/2} d\mathcal{R}_l$ and $d\mathcal{P}_M \equiv \prod_{l=-(M-1)/2}^{(M-1)/2} d\mathcal{P}_l$. Note that compared to Eq. (62) that contains integrals for all normal

modes, in $C_{AB}^{[\mathcal{M}]}$ [Eq. (70)], only the Matsubara modes are present. Furthermore, the state-independent Hamiltonian H_M , the Matsubara phase ϕ_M , and the electronic phase $\hat{\Gamma}_{\tilde{s}}^{[\mathcal{M}]}$ have the following expressions:

$$H_M = \sum_{\alpha=1}^N \mathcal{H}_0(R_\alpha^{[\mathcal{M}]}, P_\alpha^{[\mathcal{M}]}) , \quad (71a)$$

$$\phi_M = \sum_{l=-\frac{M-1}{2}}^{\frac{M-1}{2}} \mathcal{P}_l \tilde{\omega}_l \mathcal{R}_{-l} , \quad (71b)$$

$$\hat{\Gamma}_{\tilde{s}}^{[\mathcal{M}]} = \prod_{\alpha=1}^N e^{-\beta_N \frac{1}{\hbar} \sum_k \mathcal{H}_k(R_\alpha^{[\mathcal{M}]}) \cdot \hat{s}_k} \cdot \hat{w}_{\tilde{s}}^{(\alpha)} , \quad (71c)$$

where $\tilde{\omega}_l$ is the Matsubara frequency [Eq. (63)] and $\hat{w}_{\tilde{s}}^{(\alpha)}$ is the SW kernel defined in Eq. (30b) (with radius $r_{\tilde{s}}$). The Matsubara partition function Z_M is expressed as

$$\begin{aligned} Z_M &= \frac{\alpha_M}{(2\pi\hbar)^N} \int d\mathcal{R}_M \int d\mathcal{P}_M \int d\{\Omega^{(\alpha)}\} \\ &\quad \times e^{-\beta_N(H_M - iN\phi_M)} \text{Tr}_e[\hat{\Gamma}_{\tilde{s}}^{[\mathcal{M}]}] . \end{aligned} \quad (72)$$

If the operator \hat{A} is a projection operator (that only depends on the electronic DOFs), then the TCF in Eq. (62) after the Matsubara approximation is expressed as

$$\begin{aligned} C_{AB}^{[\mathcal{M}]} &= \frac{\alpha_M}{(2\pi\hbar)^N Z_M} \int d\mathcal{R}_M \int d\mathcal{P}_M \int d\{\Omega^{(\alpha)}\} \\ &\quad \times e^{-\beta_N(H_M - iN\phi_M)} \text{Tr}_e[\hat{\Gamma}_{\tilde{s}}^{[\mathcal{M}]} \hat{A}] e^{\mathcal{L}^{[\mathcal{M}]}_t} [\hat{B}]_{ws}^{[\mathcal{M}]} , \end{aligned} \quad (73)$$

with the same expressions of H_M , ϕ_M , $\hat{\Gamma}_{\tilde{s}}^{[\mathcal{M}]}$ defined in Eq. (71), and Z_M defined in Eq. (72). The trace $\text{Tr}_e[\hat{\Gamma}_{\tilde{s}}^{[\mathcal{M}]} \hat{A}]$ is expressed as

$$\begin{aligned} \text{Tr}_e[\hat{\Gamma}_{\tilde{s}}^{[\mathcal{M}]} \hat{A}] &= \frac{1}{N} \sum_{\alpha=1}^N \text{Tr}_e \left[\prod_{y \leq \alpha}^N e^{-\beta_N \frac{1}{\hbar} \sum_k \mathcal{H}_k(R_y^{[\mathcal{M}]}) \cdot \hat{s}_k} \hat{w}_{\tilde{s}}^{(y)} \right. \\ &\quad \left. \times \hat{A} \prod_{y > \alpha}^N e^{-\beta_N \frac{1}{\hbar} \sum_k \mathcal{H}_k(R_y^{[\mathcal{M}]}) \cdot \hat{s}_k} \cdot \hat{w}_{\tilde{s}}^{(y)} \right] . \end{aligned} \quad (74)$$

B. The RPMD approximation

As discussed in the previous works,^{25,30} numerically evaluating the Matsubara phase ϕ_M remains computationally challenging due to the severe sign problem. One possible way to avoid directly evaluating this phase is to make the transformation $\mathcal{P}_l \rightarrow \mathcal{P}_l - im\tilde{\omega}_l \mathcal{R}_{-l}$ together with the change in the contour of integration^{30,79} $\int_{-\infty}^{\infty} d\mathcal{P}_l \rightarrow \int_{-\infty-im\tilde{\omega}_l \mathcal{R}_{-l}}^{\infty-im\tilde{\omega}_l \mathcal{R}_{-l}} d\mathcal{P}_l$. The change of variables leads to a complex Liouvillian,

$$\mathcal{L}^{[\mathcal{M}]} \rightarrow \tilde{\mathcal{L}}^{[\mathcal{M}]} = \tilde{\mathcal{L}}_{rp}^{[\mathcal{M}]} + i\tilde{\mathcal{L}}_I^{[\mathcal{M}]} , \quad (75)$$

where $\tilde{\mathcal{L}}_{rp}^{[\mathcal{M}]}$ is the real part of the Liouvillian in the normal mode representation as follows:

$$\begin{aligned} \tilde{\mathcal{L}}_{\text{rp}}^{[\mathcal{M}]} [\hat{B}]_{\text{ws}}^{[\mathcal{M}]} &\equiv \frac{1}{\mathcal{N}} \sum_{\alpha=1}^{\mathcal{N}} \sum_{l=-\frac{\mathcal{M}-1}{2}}^{\frac{\mathcal{M}-1}{2}} \left[\left(\frac{\mathcal{P}_l}{m} \frac{\partial}{\partial \mathcal{R}_l} - m \tilde{\omega}_l^2 \mathcal{R}_l \frac{\partial}{\partial \mathcal{P}_l} \right) \right. \\ &- \frac{1}{\mathcal{N}} \left[\frac{\partial \mathcal{H}_0(R_\alpha^{[\mathcal{M}]})}{\partial \mathcal{R}_l} + r_s \sum_{j=1}^{N^2-1} \frac{\partial \mathcal{H}_j(R_\alpha^{[\mathcal{M}]})}{\partial \mathcal{R}_l} \Omega_j^{(\alpha)} \right] \frac{\partial}{\partial \mathcal{P}_l} \Big] \mathcal{B}_0^{(\alpha)[\mathcal{M}]} \\ &+ \frac{1}{\mathcal{N}} \sum_{\alpha=1}^{\mathcal{N}} \sum_{i=1}^{N^2-1} \left[\frac{r_s}{\hbar} \sum_{j,k=1}^{N^2-1} f_{ijk} \mathcal{H}_j(R_\alpha^{[\mathcal{M}]}) \Omega_k^{(\alpha)} \right] \mathcal{B}_i^{(\alpha)[\mathcal{M}]} \end{aligned} \quad (76)$$

and $i\tilde{\mathcal{L}}_1^{[\mathcal{M}]}$ is the imaginary part of the Liouvillian,^{25,30}

$$\tilde{\mathcal{L}}_1^{[\mathcal{M}]} \mathcal{B}_0^{[\mathcal{M}]} = \frac{1}{\mathcal{N}} \sum_{\alpha=1}^{\mathcal{N}} \sum_{l=-\frac{\mathcal{M}-1}{2}}^{\frac{\mathcal{M}-1}{2}} \tilde{\omega}_l \left(\mathcal{P}_l \frac{\partial}{\partial \mathcal{P}_{-l}} - \mathcal{R}_l \frac{\partial}{\partial \mathcal{R}_{-l}} \right) \mathcal{B}_0^{(\alpha)[\mathcal{M}]}.$$

Note that there is no spin mapping variable-related derivative in the above imaginary Liouvillian $\tilde{\mathcal{L}}_1^{[\mathcal{M}]}$, and its impact on the electronic dynamics should only come from its influence on the nuclear dynamics, which, in turn, couples to the electronic mapping DOFs via $\tilde{\mathcal{L}}_{\text{rp}}^{[\mathcal{M}]}$.

As discussed in Ref. 74 (Chap. 3) as well as Ref. 79, one can gradually discard the imaginary Liouvillian $i\tilde{\mathcal{L}}_1^{[\mathcal{M}]}$ in Eq. (75) and make the following approximation:

$$\tilde{\mathcal{L}}^{[\mathcal{M}]} \approx \tilde{\mathcal{L}}_{\text{rp}}^{[\mathcal{M}]} \quad (78)$$

while gradually pushing each $\int d\mathcal{P}_l$ integral toward the real axis of \mathcal{P}_l . This procedure⁷⁹ is referred to as the “RPMD approximation.” After applying the RPMD approximation, the correlation function in Eq. (70) (when \hat{A} is a linear operator of \hat{R}) is expressed as

$$C_{AB}^{[\mathcal{M}]} = \frac{\alpha_M}{(2\pi\hbar)^{\mathcal{N}} \mathcal{Z}_M} \int d\mathcal{R}_M \int d\mathcal{P}_M \int d\{\Omega^{(\alpha)}\} \times e^{-\beta_N H_{\text{rp}}^{[\mathcal{M}]}} \mathcal{A}_0(\mathcal{R}_M) \text{Tr}_e[\hat{\Gamma}_{\hat{s}}^{[\mathcal{M}]}] e^{\tilde{\mathcal{L}}_{\text{rp}}^{[\mathcal{M}]} t} [\hat{B}]_{\text{ws}}^{[\mathcal{M}]}, \quad (79)$$

where the dynamics is only evolved with $\tilde{\mathcal{L}}_{\text{rp}}^{[\mathcal{M}]}$ defined in Eq. (76), and the state-independent Hamiltonian in the initial distribution $e^{-\beta_N H_{\text{rp}}^{[\mathcal{M}]}}$ now includes the spring term of the ring-polymer as follows:

$$H_{\text{rp}}^{[\mathcal{M}]} = \sum_{\alpha=1}^{\mathcal{N}} \mathcal{H}_0(R_\alpha^{[\mathcal{M}]}, P_\alpha^{[\mathcal{M}]}) + \mathcal{N} \sum_{l=-\frac{\mathcal{M}-1}{2}}^{\frac{\mathcal{M}-1}{2}} \frac{1}{2} m \tilde{\omega}_l^2 \mathcal{R}_l^2, \quad (80)$$

where $\tilde{\omega}_l$ is the Matsubara frequency introduced in Eq. (63).

In the case of \hat{A} being a projection operator, the same approximation can be performed, and Eq. (73) becomes

$$C_{AB}^{[\mathcal{M}]}(t) = \frac{\alpha_M}{(2\pi\hbar)^{\mathcal{N}} \mathcal{Z}_M} \int d\mathcal{R}_M \int d\mathcal{P}_M \int d\{\Omega^{(\alpha)}\} \times e^{-\beta_N H_{\text{rp}}^{[\mathcal{M}]}} \text{Tr}_e[\hat{\Gamma}_{\hat{s}}^{[\mathcal{M}]} \hat{A}] e^{\tilde{\mathcal{L}}_{\text{rp}}^{[\mathcal{M}]} t} [\hat{B}]_{\text{ws}}^{[\mathcal{M}]}, \quad (81)$$

with the same $H_{\text{rp}}^{[\mathcal{M}]}$ expressed in Eq. (80) and $\tilde{\mathcal{L}}_{\text{rp}}^{[\mathcal{M}]}$ expressed in Eq. (76). The dynamics in these Kubo-transformed TCFs [Eqs. (79) and (81)] can be seen as governed by a \mathcal{N} -bead ring-polymer

$\{R_\alpha(\mathcal{R}_M)\}$ that only contains the \mathcal{M} Matsubara modes for the nuclear DOFs and \mathcal{N} mapping beads for the electronic DOFs.

C. The spin-mapping NRPMD method

Directly evaluating $C_{AB}^{[\mathcal{M}]}$ in Eqs. (79) and (81) remains numerically challenging because it often requires a large number of beads \mathcal{N} such that the total number of Matsubara modes \mathcal{M} is large enough to converge the initial quantum statistics.³⁰ This is a well-known numerical fact for the Matsubara-based path-integral molecular dynamics or Monte-Carlo approaches.⁷⁸ For the non-adiabatic case investigated here, the further complication also comes from the initial non-adiabatic phase $\text{Tr}_e[\hat{\Gamma}_{\hat{s}}^{[\mathcal{M}]}]$ [in Eq. (79)] or $\text{Tr}_e[\hat{\Gamma}_{\hat{s}}^{[\mathcal{M}]} \hat{A}]$ [in Eq. (81)], which induces a (separate) sign problem as \mathcal{N} gets very large.

We thus consider an additional approximation by replacing the Matsubara frequencies $\tilde{\omega}_l$ in Eqs. (79) and (81) with the normal mode frequencies of the ring polymer ω_l [Eq. (59)] as suggested by the original adiabatic Matsubara dynamics.³⁰ This should be viewed as a separate approximation in addition to the RPMD approximation in Sec. IV B. Expressing the TCF in the bead representation, we obtain the approximate TCF as

$$C_{AB}^{[\mathcal{N}]}(t) = \frac{1}{\mathcal{Z}_N(2\pi\hbar)^{\mathcal{N}}} \int d\{R_\alpha\} \int d\{P_\alpha\} \int d\{\Omega^{(\alpha)}\} \times e^{-\beta_N H_{\text{rp}}^{[\mathcal{N}]}} \mathcal{A}_0(R) \text{Tr}_e[\hat{\Gamma}_{\hat{s}}] e^{\mathcal{L}_{\text{rp}}^{[\mathcal{N}]} t} [\hat{B}]_{\text{ws}}, \quad (82)$$

where \hat{A} is linear in \hat{R} (or \hat{P}), and the SM-NRPMD partition function is

$$\mathcal{Z}_N = \frac{1}{(2\pi\hbar)^{\mathcal{N}}} \int d\{R_\alpha\} \int d\{P_\alpha\} \int d\{\Omega^{(\alpha)}\} e^{-\beta_N H_{\text{rp}}^{[\mathcal{N}]}} \text{Tr}_e[\hat{\Gamma}_{\hat{s}}]. \quad (83)$$

The ring-polymer Hamiltonian $H_{\text{rp}}^{[\mathcal{N}]}$ in the bead representation is expressed as

$$H_{\text{rp}}^{[\mathcal{N}]} = \sum_{\alpha=1}^{\mathcal{N}} \left[\mathcal{H}_0(R_\alpha, P_\alpha) + \frac{m}{2\beta_N^2 \hbar^2} (R_\alpha - R_{\alpha-1})^2 \right], \quad (84)$$

and the electronic phase term is

$$\hat{\Gamma}_{\hat{s}} = \prod_{\alpha=1}^{\mathcal{N}} e^{-\beta_N \frac{1}{\hbar} \sum_k \mathcal{H}_k(R_\alpha) \cdot \vec{S}_k} \cdot \hat{w}_{\hat{s}}^{(\alpha)}. \quad (85)$$

When \hat{A} is a projection operator, the TCF is expressed as

$$C_{AB}^{[\mathcal{N}]}(t) = \frac{1}{\mathcal{Z}_N(2\pi\hbar)^{\mathcal{N}}} \int d\{R_\alpha\} \int d\{P_\alpha\} \int d\{\Omega^{(\alpha)}\} \times e^{-\beta_N H_{\text{rp}}^{[\mathcal{N}]}} \text{Tr}_e[\hat{\Gamma}_{\hat{s}} \hat{A}] e^{\mathcal{L}_{\text{rp}}^{[\mathcal{N}]} t} [\hat{B}]_{\text{ws}}, \quad (86)$$

and the electronic phase $\text{Tr}_e[\hat{\Gamma}_{\hat{s}} \hat{A}]$ is expressed as

$$\begin{aligned} \text{Tr}_e[\hat{\Gamma}_{\hat{s}} \hat{A}] &= \frac{1}{\mathcal{N}} \sum_{\alpha=1}^{\mathcal{N}} \text{Tr}_e \left[\prod_{y \leq \alpha}^{\mathcal{N}} e^{-\beta_N \frac{1}{\hbar} \sum_k \mathcal{H}_k(R_y) \cdot \vec{S}_k} \hat{w}_{\hat{s}}^{(y)} \right. \\ &\quad \times \hat{A} \left. \prod_{y > \alpha}^{\mathcal{N}} e^{-\beta_N \frac{1}{\hbar} \sum_k \mathcal{H}_k(R_y) \cdot \vec{S}_k} \hat{w}_{\hat{s}}^{(y)} \right]. \end{aligned} \quad (87)$$

The Liouvillian of SM-NRPMD [see Eq. (76)] in the bead representation is expressed as

$$\begin{aligned} \mathcal{L}_{\text{rp}}^{[N]}[\hat{B}]_{\text{ws}} = & \frac{1}{N} \sum_{\alpha=1}^N \left[\frac{P_\alpha}{m} \frac{\partial}{\partial R_\alpha} - \frac{m}{\beta_N^2 \hbar^2} (2R_\alpha - R_{\alpha-1} - R_{\alpha+1}) \frac{\partial}{\partial P_\alpha} \right. \\ & - \left[\frac{\partial H_0(R_\alpha)}{\partial R_\alpha} + r_s \sum_{j=1}^{N^2-1} \frac{\partial H_j(R_\alpha)}{\partial R_\alpha} \Omega_j^{(\alpha)} \right] \frac{\partial}{\partial P_\alpha} \Big] \mathcal{B}_0^{(\alpha)} \\ & + \frac{1}{N} \sum_{\alpha=1}^N \sum_{i=1}^{N^2-1} \left[\frac{r_s}{\hbar} \sum_{j,k=1}^{N^2-1} f_{ijk} H_j(R_\alpha) \Omega_k^{(\alpha)} \right] \mathcal{B}_i^{(\alpha)}, \quad (88) \end{aligned}$$

where $\mathcal{B}_0^{(\alpha)}$ and $\mathcal{B}_i^{(\alpha)}$ are defined in Eq. (48).

The Liouvillian in Eq. (88) leads to the SM-NRPMD Hamiltonian as follows:

$$\begin{aligned} \mathcal{H}_N = & \sum_{\alpha=1}^N \left[H_0(R_\alpha, P_\alpha) + \frac{m}{2\beta_N^2 \hbar^2} (R_\alpha - R_{\alpha-1})^2 + \sum_{i=1}^{N^2-1} r_s \mathcal{H}_i(R_\alpha) \Omega_i^{(\alpha)} \right] \\ = & H_{\text{rp}}^{[N]} + \sum_{\alpha=1}^N \sum_{i=1}^{N^2-1} r_s \mathcal{H}_i(R_\alpha) \Omega_i^{(\alpha)}, \quad (89) \end{aligned}$$

where H_0 is expressed in Eq. (50b) and $H_{\text{rp}}^{[N]}$ is expressed in Eq. (E6).

The EOMs for the SM-NRPMD method based on the Liouvillian in Eq. (88) are

$$\dot{R}_\alpha = \frac{P_\alpha}{m}, \quad (90a)$$

$$\dot{P}_\alpha = -\frac{\partial H_{\text{rp}}^{[N]}}{\partial R_\alpha} - r_s \sum_{i=1}^{N^2-1} \frac{\partial \mathcal{H}_i}{\partial R_\alpha} \cdot \Omega_i^{(\alpha)}, \quad (90b)$$

$$\dot{\Omega}_i^{(\alpha)} = \frac{1}{\hbar} \sum_{j,k=1}^{N^2-1} f_{ijk} H_j(R_\alpha) \cdot \Omega_k^{(\alpha)}, \quad (90c)$$

which are the Hamilton's EOMs of the Hamiltonian \mathcal{H}_N in Eq. (89). This can be viewed as the ring-polymer version of the linearized spin mapping EOMs derived in Ref. 51, as well as generalization of the spin precession to N -dimensions with $SU(N)$ symmetry⁵⁸ introduced by Hioe and Eberly (without the presence of any nuclear DOF).

The correlation function in Eqs. (82) and (86) and the Liouvillian $\mathcal{L}_{\text{rp}}^{[N]}$ in Eq. (88) constitute the SM-NRPMD approach to compute Kubo-transformed TCFs. The approximations we have made to obtain this expression are (1) Matsubara approximation [Eq. (65)], (2) ignoring the $\mathcal{L}_i^{n(\alpha)}$ term [Eq. (60c)] in EOMs, (3) the RPMD approximation [Eq. (78)], (4) replacing the Matsubara frequencies [Eq. (63)] with the normal mode frequencies of the ring polymer [Eq. (59)] in the correlation function expression. Approximations (1), (3), and (4) are related to the original derivation of the adiabatic version of RPMD, whereas approximation (2) is related specifically to the SM-NRPMD approach.

There are several interesting connections between the current SM-NRPMD formalism and previous works. First, for the two-level special case ($N = 2$), both the EOMs and the Kubo-transformed TCF of the current formalism reduce back to those proposed in our previous work.⁵² Note that in Ref. 52 the initial distribution (partition function) was derived based on the imaginary-time path-integral approach and the dynamics were proposed. Here, the Kubo-transformed TCF and dynamics are derived based on the Matsubara

approximation and the RPMD approximation of the exact TCF. The main equations of SM-NRPMD for the two-state special case are provided in Appendix D. Second, in the one-bead limit, $N = 1$, the Hamiltonian \mathcal{H}_N [Eq. (89)] and the corresponding EOMs in Eq. (90) reduce back to the same expressions for the linearized spin mapping dynamics^{44,51} [Eq. (86) in Ref. 51] for a regular TCF. Third, under the state-independent limit or the electronically adiabatic limit (such that the ground electronic state is well separated from other electronic states), this formalism reduces back to the original adiabatic RPMD.^{5,80} Finally, when choosing only one bead for the nuclear DOF and N beads for the electronic mapping DOFs, the current formalism is closely connected to the recently proposed spin mapping path-integral approach.⁸¹

Note that under the $t \rightarrow 0$ limit, Eq. (86) becomes

$$\begin{aligned} C_{AB}^{[N]}(0) = & \frac{1}{Z_N(2\pi\hbar)^N} \int d\{R_\alpha\} \int d\{P_\alpha\} \int d\{\Omega^{(\alpha)}\} \\ & \times e^{-\beta_N H_{\text{rp}}^{[N]}} \text{Tr}_e[\hat{\Gamma}_s \hat{A}] [\hat{B}]_{\text{ws}}. \quad (91) \end{aligned}$$

This expression can also be obtained from a standard imaginary-time path-integral technique,^{52,82} which will be exact under the $N \rightarrow \infty$ limit.⁵² The two-state system ($N = 2$) example for such a derivation is provided in our previous work,⁵² which is referred to as the spin coherent state (SCS) partition function [Eq. (35) in Ref. 52]. The difference between the path-integral derivation and the Matsubara derivation is that the Matsubara dynamics introduce the nuclear momenta from a multidimensional Wigner transform [Eq. (36)], which can be viewed as the physical momenta, whereas the imaginary-time path-integral approach introduces these nuclear momenta as fictitious variables. More of this discussion can be found in Eq. (79) of Ref. 25.

The original adiabatic version of RPMD has a desirable property, which preserves quantum Boltzmann distribution and the detailed balance, $\langle \hat{A}(t) \rangle = \langle \hat{A}(0) \rangle$. The key to achieve the detailed balance condition is

$$\mathcal{L}_{\text{rp}}^{[N]} \left(K_n^{(\alpha)} e^{-\beta_N H_{\text{rp}}^{[N]}} \text{Tr}_e[\hat{\Gamma}_s] \right) = 0, \quad (92)$$

where $K_n^{(\alpha)}$ is the Jacobian determinant [see Eq. (B4)] in the differential phase space volume element $\int d\{\Omega^{(\alpha)}\}$. Unfortunately, due to the complexity of the distribution, which includes an electronic trace [Eq. (85)], we do not have an analytical proof of Eq. (92). Nevertheless, in our previous work on SM-NRPMD in the two-state special case, we have shown that the expectation values of position and population are conserved for a sufficiently large number of beads (Fig. 4 of Ref. 52).

It is also possible to simulate non-equilibrium TCF with SM-NRPMD, similar to the case of the MMST version of NRPMD, as discussed in Ref. 25. In Appendix E, we provide details on how to compute the time-dependent reduced density matrix dynamics upon photo-excitation.

D. Equations of motion in the Cartesian mapping variables

There are multiple ways to write the EOMs using various conjugated mapping variables.^{44,51} To simplify the expression of the EOMs and reduce the number of mapping variables, one can express

the mapping variables $\Omega^{(\alpha)}$ [in Eq. (30c)] as Cartesian mapping variables. This can be accomplished by representing the expansion coefficients of the spin coherent states in Eq. (7) by their real and imaginary parts^{44,83} for every copy (α -bead) of the coherent state as follows:

$$\langle n|\Omega^{(\alpha)}\rangle \cdot e^{i\Phi^{(\alpha)}} = \frac{1}{\sqrt{2r_s}}(q_n^{(\alpha)} + ip_n^{(\alpha)}), \quad (93)$$

where $q_n^{(\alpha)}/\sqrt{2r_s}$ is the real part of the expansion coefficients, $p_n^{(\alpha)}/\sqrt{2r_s}$ is the imaginary part of the expansion coefficients, and $e^{i\Phi^{(\alpha)}}$ is a *constant global phase* to all of the coefficients $\langle n|\Omega^{(\alpha)}\rangle$ associated with the α th copy of the coherent state $|\Omega^{(\alpha)}\rangle$. The above relation provides a canonical transformation from the previously defined spin-mapping variables $\{\Omega_k^{(\alpha)}\}$ to a set of Cartesian mapping variables,

$$\begin{aligned} 2r_s\Omega_k^{(\alpha)} &= 2r_s\langle\Omega^{(\alpha)}|\hat{S}_k|\Omega^{(\alpha)}\rangle \\ &= \sum_{n,m}\langle n|\hat{S}_k|m\rangle \cdot (q_m^{(\alpha)} - ip_m^{(\alpha)})(q_n^{(\alpha)} + ip_n^{(\alpha)}). \end{aligned} \quad (94)$$

Using this transform [Eq. (94)], the estimator of the projection operator [Eq. (46)] becomes

$$[|n\rangle\langle m|]_s^{(\alpha)} = \frac{1-r_s}{N}\delta_{nm} + \frac{1}{2}(q_m^{(\alpha)} + ip_m^{(\alpha)})(q_n^{(\alpha)} - ip_n^{(\alpha)}), \quad (95)$$

with the details presented in Appendix D [Eqs. (D7)–(D10)] of Ref. 51.

The Hamiltonian in Eq. (89) can be transformed to Cartesian variables as follows:

$$\begin{aligned} H_N &= \sum_{\alpha=1}^N \left[\mathcal{H}_0(R_\alpha, P_\alpha) + \frac{m}{2\beta_N^2 \hbar^2} (R_\alpha - R_{\alpha-1})^2 + \sum_{n=1}^N [V_{nn}(R_\alpha) - \bar{V}(R_\alpha)] \right. \\ &\quad \times \left. \frac{1}{2}([q_n^{(\alpha)}]^2 + [p_n^{(\alpha)}]^2 - \gamma) + \sum_{n < m} V_{nm}(R_\alpha)(q_n^{(\alpha)} q_m^{(\alpha)} + p_n^{(\alpha)} p_m^{(\alpha)}) \right], \end{aligned} \quad (96)$$

where $\bar{V}(R_\alpha) \equiv \frac{1}{N} \sum_{n=1}^N V_{nn}(R_\alpha)$ and the effective zero-point energy (ZPE) parameter is^{44,51}

$$\gamma = 2(r_s - 1)/N. \quad (97)$$

The expression of H_N in Eq. (96) is equivalent to the MMST version of the NRPMD Hamiltonian (when choosing $\gamma = 1$), which was originally proposed in Ref. 11 and later justified in Ref. 25. Note that even with the Hamiltonian being identical, the derivation of H_N is based on the $SU(N)$ mapping outlined in Sec. IV C and is not based on the MMST mapping formalism.^{28,29} The fundamental differences between the two mapping formalism are discussed in Appendix D of Ref. 51.

In terms of the Cartesian mapping variables, $\{q_n^{(\alpha)}, p_n^{(\alpha)}\}$, the corresponding EOMs in Eq. (90) are transformed as⁴⁴

$$\dot{R}_\alpha = \frac{P_\alpha}{m}, \quad (98a)$$

$$\begin{aligned} \dot{P}_\alpha &= -\frac{\partial \mathcal{H}_{rp}^{[N]}}{\partial R_\alpha} - \sum_{n=1}^N \frac{\partial(V_{nn} - \bar{V})}{\partial R_\alpha} \frac{1}{2}([q_n^{(\alpha)}]^2 + [p_n^{(\alpha)}]^2 - \gamma) \\ &\quad - \sum_{n < m} \frac{\partial V_{nm}}{\partial R_\alpha} (q_n^{(\alpha)} q_m^{(\alpha)} + p_n^{(\alpha)} p_m^{(\alpha)}), \end{aligned} \quad (98b)$$

$$\dot{q}_n^{(\alpha)} = \sum_{m=1}^N V_{nm} p_m^{(\alpha)}, \quad (98c)$$

$$\dot{p}_n^{(\alpha)} = -\sum_{m=1}^N V_{nm} q_m^{(\alpha)}, \quad (98d)$$

where $V_{nm}(R_\alpha)$ is defined in Eq. (1) and $\mathcal{H}_{rp}^{[N]}$ is expressed in Eq. (E6). The above EOMs are indeed the Hamilton's EOMs of H_N in Eq. (96).

V. COMPUTATIONAL DETAILS

Summary of the SM-NRPMD approach. The SM-NRPMD approach computes the Kubo-transformed TCF for $\hat{A} = \hat{R}$ (or any linear nuclear operator) based upon Eq. (82) and for $\hat{A} = |n\rangle\langle n|$ (or any projection operator) using Eq. (86). The initial distribution of the nuclear variables $\{R_\alpha, P_\alpha\}$ and the mapping variables $\{\theta_n^{(\alpha)}, \varphi_n^{(\alpha)}\}$ (see Appendix B) are governed by the initial distribution

$$d\{R_\alpha\} d\{P_\alpha\} d\{\Omega^{(\alpha)}\} e^{-\beta_N H_{rp}^{[N]}} \text{Tr}_e[\hat{F}_s]$$

for Eq. (82) and

$$d\{R_\alpha\} d\{P_\alpha\} d\{\Omega^{(\alpha)}\} e^{-\beta_N H_{rp}^{[N]}} \text{Tr}_e[\hat{F}_s \hat{A}]$$

for Eq. (86), with each $d\Omega^{(\alpha)}$ expressed in Eq. (B4) (with $\{\theta_n^{(\alpha)}, \varphi_n^{(\alpha)}\}$). Note that $K_n^{(\alpha)}$ in Eq. (B4) (which is a function of $\{\theta_n^{(\alpha)}\}$) needs to be included in the sampling function for an efficient numerical convergence. The electronic quantities $\text{Tr}_e[\hat{F}_s]$ and $\text{Tr}_e[\hat{F}_s \hat{A}]$ are, in general, complex.

The dynamics are propagated using the EOMs in Eq. (98). These EOMs are identical to the original MMST-based NRPMD approach.^{11,12,25} Thus, one can take advantage of using the existing algorithms^{12,40} for integrating these EOMs. Because the initial conditions are sampled with $\{\varphi_n^{(\alpha)}, \theta_n^{(\alpha)}\}$, these variables are transformed into the Cartesian mapping variables, $\{q_n^{(\alpha)}, p_n^{(\alpha)}\}$, for the dynamics propagation. This can be done based on Eq. (93) as follows:

$$q_n^{(\alpha)} = \sqrt{2r_s} \cdot \text{Re}[\langle n|\Omega^{(\alpha)}\rangle \cdot e^{i\Phi^{(\alpha)}}], \quad (99a)$$

$$p_n^{(\alpha)} = \sqrt{2r_s} \cdot \text{Im}[\langle n|\Omega^{(\alpha)}\rangle \cdot e^{i\Phi^{(\alpha)}}], \quad (99b)$$

where the explicit expression of $\langle n|\Omega^{(\alpha)}\rangle$ as a function of $\{\theta_n^{(\alpha)}, \varphi_n^{(\alpha)}\}$ can be found in Eq. (B1) (for all α). The correlation function can then be explicitly calculated through trajectory average. The global phase $e^{i\Phi^{(\alpha)}}$ does not influence the results. For the results presented in this

work, we use a particular Bloch sphere radius (referred to as the W method^{44,51}),

$$r_s = r_{\bar{s}} = \sqrt{N+1}. \quad (100)$$

This choice has shown to give the overall most accurate results for linearized method⁴⁴ as well as for the two level case for SM-NRPMD⁵² compared to other radii.

Numerical algorithm to perform SM-NRPMD simulations. The SM-NRPMD method evaluates the Kubo-transformed TCFs expressed in Eqs. (82) or (86). The initial distribution is obtained using the Metropolis algorithm^{84,85} with the nuclear variables $\{R_\alpha, P_\alpha\}$ and the mapping variables $\{\theta^{(\alpha)}, \varphi^{(\alpha)}\}$ as those define the initial phase space. The Metropolis algorithm requires a positive-definite sampling function. As done previously,^{11,14,25,39,52} the absolute value of the initial distribution is sampled and the remaining phase is included in the estimator. The distribution function used for sampling is chosen to be

$$\rho_{\bar{s}}(\{R_\alpha, P_\alpha, \theta^{(\alpha)}, \varphi^{(\alpha)}\}) = \left[\prod_{\alpha=1}^N \prod_{n=1}^{N-1} K_n^{(\alpha)} \right] \cdot e^{-\beta_N H_{\text{tp}}^{[\mathcal{N}]}} [\text{Tr}_e[\hat{\Gamma}_{\bar{s}}]], \quad (101)$$

where the elements $K_n^{(\alpha)}$ [which are functions of $(\theta_n^{(\alpha)})$] are expressed in Eq. (B4) and $\hat{\Gamma}_{\bar{s}}$ is expressed in Eq. (85). In $\rho_{\bar{s}}$, every quantity is expressed in terms of $\{R_\alpha, P_\alpha\}$ and $\{\theta^{(\alpha)}, \varphi^{(\alpha)}\}$. The expression of $\hat{\Gamma}_{\bar{s}}$ [Eq. (85)] contains the SW kernel $\hat{w}_{\bar{s}}^{(\alpha)}$ [Eq. (17b)] as a function of $\{\Omega_k^{(\alpha)}\}$. These $\{\Omega_k^{(\alpha)}\}$ are also functions of $\{\theta^{(\alpha)}, \varphi^{(\alpha)}\}$, with the detailed expressions in Eqs. (B5)–(B7) in Appendix B.

Using the absolute value of $\text{Tr}_e[\hat{\Gamma}_{\bar{s}}]$ as part of the distribution $\rho_{\bar{s}}$, the remaining phase associated with $\text{Tr}_e[\hat{\Gamma}_{\bar{s}}]$ is expressed as

$$\Xi_{\bar{s}}(\{R_\alpha, P_\alpha, \theta^{(\alpha)}, \varphi^{(\alpha)}\}) = \frac{\text{Tr}_e[\hat{\Gamma}_{\bar{s}}]}{|\text{Tr}_e[\hat{\Gamma}_{\bar{s}}]|}, \quad (102)$$

which has to be included as part of the estimator when computing ensemble averages [see Eq. (103)]

To propagate the dynamics, the spin-mapping variables $\{\theta^{(\alpha)}, \varphi^{(\alpha)}\}$ (generalized Euler angles) are converted into the Cartesian variables $\{\mathbf{p}^{(\alpha)}, \mathbf{q}^{(\alpha)}\}$ after the initial sampling governed by $\rho_{\bar{s}}$ [Eq. (101)]. The global phase is chosen to be $\Phi^\alpha = 0$ for all initially sampled configurations. Specifically, we use the normal mode integrator⁸⁶ to solve the ring-polymer part of the EOMs in Eqs. (98a) and (98b) and the symplectic integrator for the mapping variables^{40,87} in Eqs. (98c) and (98d). Note that a simple Verlet algorithm¹² with a sufficiently small time-step to propagate the mapping variables gives an identical result.

The Kubo-transformed nuclear position auto-correlation function is obtained by choosing $\hat{A} = \hat{B} = \hat{R}$. The SM-NRPMD approximation is evaluated as

$$C_{RR}^{[\mathcal{N}]}(t) = \frac{\langle \text{Re}\{\Xi_{\bar{s}}\} \bar{R}(0) \bar{R}(t) \rangle}{\langle \text{Re}\{\Xi_{\bar{s}}\} \rangle}, \quad (103)$$

where $\bar{R} = \frac{1}{N} \sum_{\alpha=1}^N R_\alpha$. The brackets $\langle \dots \rangle$ indicate an ensemble average according to the initial distribution governed by $\rho_{\bar{s}}$. Only the real part of the phase estimator in Eq. (102) is included as the estimator because the correlation function is purely real.

We also consider $\hat{A} = |m\rangle\langle m|$ and $\hat{B} = |n\rangle\langle n|$ for the Kubo-transformed TCF of population. The SM-NRPMD approximation of this TCF is

$$C_{mn}^{[\mathcal{N}]}(t) = \frac{\langle \text{Re}\{\xi_{\bar{s}}\} [|n\rangle\langle n|]_s(t) \rangle}{\langle \text{Re}\{\Xi_{\bar{s}}\} \rangle}, \quad (104)$$

where the initial distribution function is always $\rho_{\bar{s}}$ in Eq. (101) and

$$\xi_{\bar{s}}(\{R_\alpha, P_\alpha, \theta^{(\alpha)}, \varphi^{(\alpha)}\}) = \frac{\text{Tr}_e[\hat{\Gamma}_{\bar{s}} |m\rangle\langle m|]}{|\text{Tr}_e[\hat{\Gamma}_{\bar{s}}]|}, \quad (105)$$

where $\text{Tr}_e[\hat{\Gamma}_{\bar{s}} |m\rangle\langle m|]$ is evaluated using the expression in Eq. (87) (with $\hat{A} = |m\rangle\langle m|$), and the time-evolved projection operator [Eq. (45)] is evaluated [based on Eq. (95)] as follows:

$$[|n\rangle\langle n|]_s(t) = \frac{1}{\mathcal{N}} \sum_{\alpha=1}^{\mathcal{N}} \frac{1}{2} \left([q_n^{(\alpha)}(t)]^2 + [p_n^{(\alpha)}(t)]^2 - \gamma \right), \quad (106)$$

where γ is defined in Eq. (97).

Model Systems. The accuracy of SM-NRPMD dynamics for $N = 2$ special case has already been extensively tested in our previous work.⁵² In this work, we focus on $N = 3$ model systems with electronic coupling parameters Δ , ranging from electronically adiabatic regime ($\beta\Delta \gg 1$) to non-adiabatic regime ($\beta\Delta \ll 1$). The model contains three diabatic electronic states $|1\rangle$, $|2\rangle$, and $|3\rangle$, as well as one nuclear DOF \hat{R} , with the Hamiltonian expressed as

$$\hat{H} = \frac{\hat{P}^2}{2m} + \frac{1}{2} m\omega\hat{R}^2 + \begin{pmatrix} k_1\hat{R} + \epsilon_1 & \Delta_{12} & 0 \\ \Delta_{12} & k_2\hat{R} + \epsilon_2 & \Delta_{23} \\ 0 & \Delta_{23} & k_3\hat{R} + \epsilon_3 \end{pmatrix} \equiv \frac{\hat{P}^2}{2m} + \hat{V}. \quad (107)$$

In this model, state $|2\rangle$ is coupled to state $|1\rangle$ and state $|3\rangle$, but there is no direct electronic coupling between state $|1\rangle$ and $|3\rangle$. This model is similar to a charge transfer model from donor state to acceptor state, with a bridge state mediating the charge transfer process. We set $\hbar = \omega = \beta = 1$. Three sets of parameters are considered in this work, which are summarized in Table I and referred to as Models I–III.

Computational Details. All the simulations presented here require $\mathcal{N} = 6$ beads for converged results. The nuclear time-step

TABLE I. Parameters for the three-state model (in a.u.).

Parameter	Model I	Model II	Model III
m	1.0	1.0	2.0
k_1	1.0	2.0	2.0
k_2	-1.0	-1.0	0.0
k_3	2.0	0.0	-2.0
ϵ_1	0.0	0.0	0.0
ϵ_2	0.0	0.0	-2.5
ϵ_3	0.0	0.0	0.0
Δ_{12}	10.0	5.0	0.5
Δ_{23}	10.0	1.0	0.5

used in all the simulations is $\Delta t = 10^{-2}$ a.u., and the electronic time-step for the mapping variables is $dt = \Delta t/10$. To obtain converged results, a total of 5×10^5 trajectories is used for the $C_{RR}^{[N]}(t)$ calculations for model I, and up to 5×10^6 trajectories are required for model II and 10^7 for model III. The population correlation function $C_{mn}^{[N]}(t)$ requires 5–10 times more trajectories to converge compared to the $C_{RR}^{[N]}(t)$ calculations for each model systems.

We present numerical comparisons between the SM-NRPMD approach and the previously proposed MMST-based NRPMD method¹¹ and benchmark against the exact calculation of the Kubo-transformed TCF, with the details of these other two approaches provided in Appendix F. The numerical convergence of the MMST-based NRPMD method¹¹ is similar to that of SM-NRPMD. For both of the NRPMD approaches, it requires more trajectories to converge the three-level model systems studied here compare to the two-level systems investigated previously¹¹ due to the more severe sign problem in the $\text{Tr}_e[\hat{\Gamma}_{\hat{s}}]$ term for $N = 3$ compared to the case of $N = 2$.

We want to emphasize that this sign problem related to $\text{Tr}_e[\hat{\Gamma}_{\hat{s}}]$ (which has both positive and negative contribution) is common for all state-dependent RPMD methods, including the mean-field RPMD,¹⁰ MV-RPMD,¹⁴ and the MMST versions of NRPMD.^{11,12} This sign problem due to $\text{Tr}_e[\hat{\Gamma}_{\hat{s}}]$ is highly system dependent (less prominent for the adiabatic regime than the non-adiabatic regime) and will become more severe as the system has more states. It is, however, possible if one wants to use the SM-NRPMD method for a given system, to first only compute the initial distribution, without propagating the dynamics, and to estimate if a severe sign problem appears (meaning that many trajectories will be necessary to converge the results). This can be done by using a small batch of trajectories and comparing the ensemble average of the sign of $\text{Tr}_e[\hat{\Gamma}_{\hat{s}}]$, given by $\langle \text{Re}\{\Xi_{\hat{s}}\} \rangle$, to the total number of trajectories. The statistics required will be higher if the first number is much smaller than the second. Another interesting numerical observation is that the numerical convergence is faster for a nuclear observable (like the nuclear position) than for population dynamics. Thus, the SM-NRPMD approach is more efficient to compute correlation functions, such as the flux-side correlation function (which gives the rate constant), using a nuclear position-related dividing surface.

VI. RESULTS AND DISCUSSION

Figure 1 presents the results of the Kubo-transformed TCF for model I. This model is in the electronically adiabatic regime ($\beta\Delta_{12} = \beta\Delta_{23} \gg 1$). The top panel depicts the diagonal potential $V_{nn} = \langle n | \hat{V} | n \rangle$ with \hat{V} defined in Eq. (107). The bottom left panel presents the auto-correlation function of the nuclear position operator $C_{RR}^{[N]}(t)$, computed using the SM-NRPMD approach (black solid line) and the numerically exact result (red dots). The result of the MMST-based NRPMD approach is visually identical to the result of SM-NRPMD and, thus, is not shown here. The bottom right panel presents the population correlation functions $C_{21}^{[N]}(t)$ (red), $C_{22}^{[N]}(t)$ (blue), and $C_{23}^{[N]}(t)$ (green), obtained with SM-NRPMD (solid lines) and numerically exact simulations (filled circles). The MMST-based NRPMD approach is also visually identical to the results of SM-NRPMD. Similar to the previous studies for two level systems,¹¹ under the electronically adiabatic

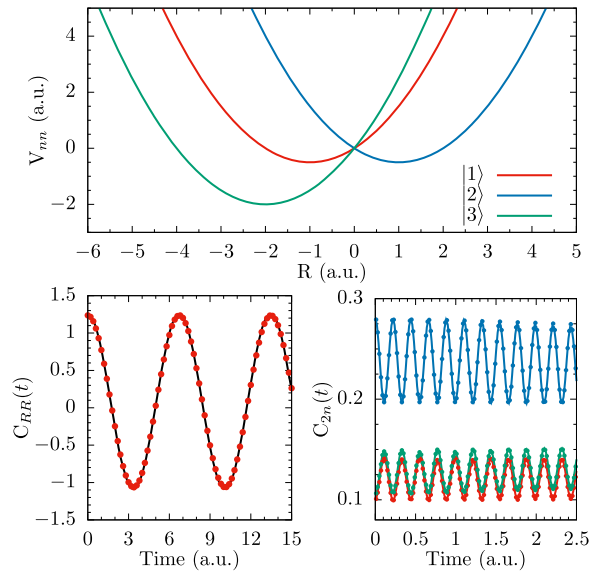


FIG. 1. Top panel: the diagonal potential $V_{nn} = \langle n | \hat{V} | n \rangle$ of model I, with \hat{V} defined in Eq. (107). Bottom left panel: Kubo-transformed position auto-correlation function obtained from SM-NRPMD (black solid line) compared to the numerically exact result (red dots). Bottom right panel: Kubo-transformed electronic population correlation functions, $C_{21}^{[N]}(t)$ (red), $C_{22}^{[N]}(t)$ (blue), and $C_{23}^{[N]}(t)$ (green), obtained with SM-NRPMD (solid lines) and compared to exact results (dots). The results from MMST-NRPMD are indistinguishable with the SM-NRPMD and, thus, not presented here.

limit, SM-NRPMD agrees with the exact answer. Furthermore, the SM-NRPMD approach provides accurate initial quantum statistics [exact value of $C_{AB}^{[N]}(0)$] as well as the correct electronic Rabi oscillations in $C_{mn}^{[N]}(t)$.

Figure 2 presents the results for model II, where $\beta\Delta_{12} > 1$ (adiabatic limit) and $\beta\Delta_{23} = 1$ (intermediate regime). The top panel depicts the diagonal potential V_{nn} . The bottom panels present the $C_{RR}^{[N]}(t)$ obtained from SM-NRPMD (bottom left) and the MMST-based NRPMD (bottom right). The dynamics are reproduced at early times by SM-NRPMD (bottom left) and matches the exact result. For a longer time (for $t > 6$ a.u.), the SM-NRPMD dynamics starts to deviate from the exact answer but remain accurate. On the other hand, NRPMD (bottom right) is only able to accurately capture the dynamics for a very short time. The magnitude of the oscillations of the NRPMD approach dampens and the auto-correlation function remains positive, whereas the exact result oscillates around zero.

Figure 3 presents the population correlation functions of model II. Although both SM-NRPMD and NRPMD are able to capture the basic features of the exact dynamics, there are deviations between them with the exact results. Nevertheless, SM-NRPMD is more accurate than NRPMD, where the latter deviates from the correct value in panel (b) for $C_{21}^{[N]}(t)$ (red) and $C_{22}^{[N]}(t)$ (blue) although the coupling Δ_{12} is under the adiabatic regime $\beta\Delta_{12} > 1$. This deviation is likely due to the presence of the other intermediate coupling Δ_{23} , and the NRPMD approach is less accurate to describe dynamics when mediated by such an intermediate state. This deviation was also seen

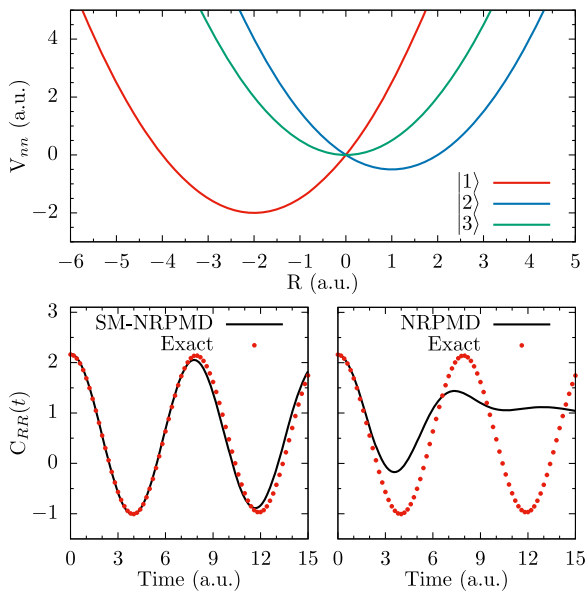


FIG. 2. Top: the diagonal potential V_{nn} of Model II. Bottom left panel: auto-correlation function of position obtained with SM-NRPMD (black solid line) compared to exact result (red dots). Bottom right panel: auto-correlation function of position obtained with NRPMD (solid lines).

on the position auto-correlation function in the bottom right panel of Fig. 2. Panels (c) and (d) show $C_{32}^{[N]}(t)$, which present a correlation between the population of states $|2\rangle$ and $|3\rangle$, where the electronic coupling between them is in the intermediate regime ($\beta\Delta_{23} = 1$). In

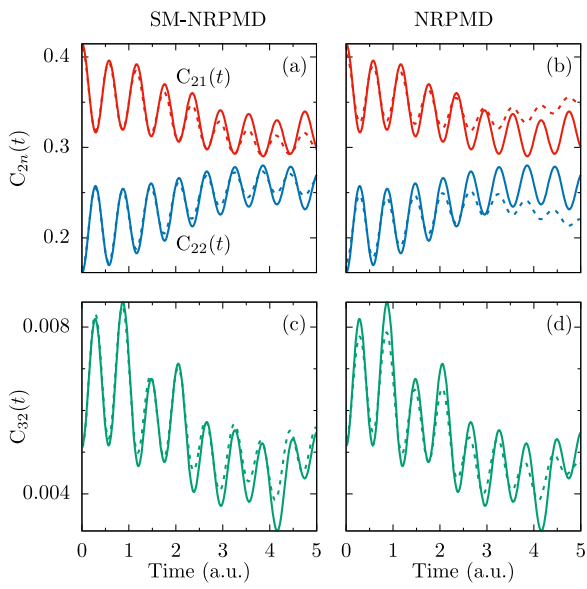


FIG. 3. Kubo-transformed population TCF (a) and (b) $C_{21}^{[N]}(t)$ (red) and $C_{22}^{[N]}(t)$ (blue) as well as $C_{32}^{[N]}(t)$ (green) for model II. Results are obtained with SM-NRPMD [dashed lines in panels (a) and (c)] and NRPMD [dashed lines in panels (b) and (d)] compared with exact calculations (solid lines).

this case, the early dynamics is exactly reproduced by SM-NRPMD, but NRPMD is underestimating the oscillation magnitude for $t < 0.5$ a.u. At longer times, both methods overly dampen the oscillation magnitudes compared to the exact results.

Figure 4 presents the results for model III, with the diagonal potential presented in the top panel. Model III is under the electronically non-adiabatic regime ($\beta\Delta_{12} = \beta\Delta_{23} < 1$). This model is numerically challenging for both trajectory-based methods, similar to the previously investigated two-level systems under the same regime.^{11,14} Both SM-NRPMD (bottom left) and NRPMD (bottom right) are unable to reproduce the dynamics exactly except at short times. While the NRPMD results quickly deviate from the exact answer (bottom right), SM-NRPMD (bottom left) provides a much better agreement of the period of oscillation for the correlation function, and only deviates slightly from the exact answer in terms of the oscillation amplitude. All the numerical results demonstrate that SM-NRPMD provides more accurate dynamics compared to the original NRPMD approach.¹¹

It is interesting to note that the numerical differences of the Kubo-transformed TCF obtained from SM-NRPMD and NRPMD are much larger for the three-state models studied here than for the two-state models studied in our previous work on SM-NRPMD.⁵² This is likely due to the fact that the difference between the symmetry of the subspace of the quantum system and the mapping subspace for three-state systems [$\otimes_3 SU(2)$ for the MMST mapping subspace and $SU(3)$ for the spin mapping subspace] is larger than for a two-state system [$\otimes_2 SU(2)$ vs $SU(2)$]. The incorrect MMST subspace is further away from the original subspace for a larger number of states, explaining larger errors in the results when increasing the number of states.

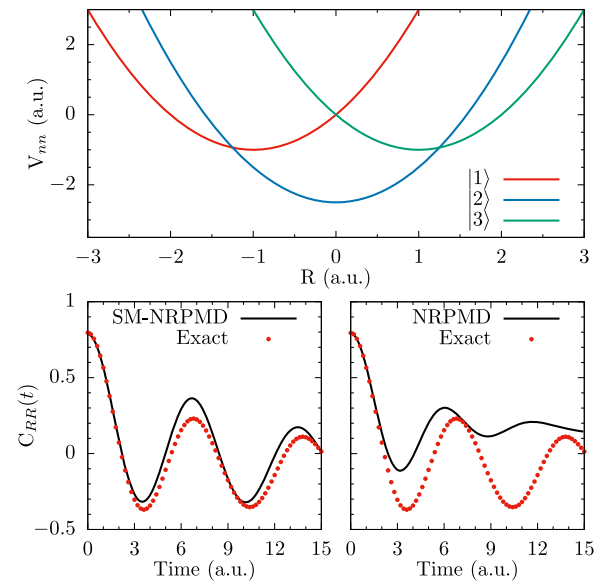


FIG. 4. Top: the diagonal potential V_{nn} of model III. Bottom left panel: Kubo-transformed auto-correlation function of position obtained with SM-NRPMD (black solid line) compared to exact result (red dots). Bottom right panel: auto-correlation function obtained with NRPMD (solid lines).

Finally, we want to comment on the potential advantage of the SM-NRPMD approach compared to the spin-LSC approach.^{43,44,51} Both approaches use the spin mapping formalism. The main difference is that SM-NRPMD uses the ring polymer quantization to describe the nuclear dynamics, whereas the spin-LSC approach uses the Wigner distribution and classical EOMs to describe nuclear dynamics (due to the linearization of the regular TCF, as shown in Ref. 51). It is a well-known fact that the ring polymer description of the nuclei does not suffer from severe zero-point energy leakage problem,^{80,88} whereas the LSC-based approaches, on the other hand, does severely suffer from the ZPE leakage⁸⁸ due to the fact that the classical EOMs do not preserve the initial Wigner distribution, in general. This has already been shown in the case of non-equilibrium dynamics on polariton-mediated electron transfer (PMET) simulations²⁶ using the MMST-based NRPMD and MMST-based LSC (see Figs. S1 and S6 of the supplementary material in Ref. 26). We expect this to also happen for the SM-based approaches, which are subject to future investigations.

VII. CONCLUSION

In this work, we derive the SM-NRPMD method for a general N -level system. Our formalism is based on the Kubo-transformed time correlation function (TCF). We use the spin-mapping representation and Stratonovich–Weyl transform that map the electronic DOFs onto continuous variables in the phase space of $SU(N)$ Lie group, which explicitly addresses the known challenges^{44,51} in the original MMST mapping formalism.^{28,29} We then use the multidimensional Wigner transform to describe the nuclear DOFs in the Kubo-transformed TCF. We further derive the spin mapping non-adiabatic Matsubara dynamics using the Matsubara approximation that removes the high frequency nuclear normal modes in the TCF. Furthermore, discarding the imaginary part of the Liouvillian (i.e., the RPMD approximation) from the non-adiabatic Matsubara dynamics, we derive the expression of the SM-NRPMD method. The two-state special case of SM-NRPMD was first proposed in Ref. 52. For the one bead limit, the EOMs of the SM-NRPMD method reduce back to the EOMs used in the spin-LSC method for a regular TCF. Even though the EOMs for SM-NRPMD [Eq. (98)] are formally identical to those of the MMST-based NRPMD,^{11,25} the initial distribution of the mapping variables [see Eq. (101) for SM-NRPMD and Eq. (F1) for NRPMD] and the choice of zero-point energy parameters, or rather of Bloch sphere radius [Eq. (97) for SM-NRPMD and $\gamma = 1$ for NRPMD¹¹], are indeed different.

We use numerical simulations to demonstrate the accuracy of the SM-NRPMD approach, with a three-state system coupled to one nuclear DOF, with the electronic couplings ranging from adiabatic to the non-adiabatic limit. Using the SM-NRPMD approach, we computed the Kubo-transformed nuclear position auto-correlation function and population time-correlation functions. The results generated from SM-NRPMD are very accurate compared to the numerically exact simulations in all parameter regimes and provide a significant improvement compared to the NRPMD method. Future applications of SM-NRPMD could be computing rate constants for non-adiabatic systems based on the flux-side correlation function formalism,^{18,89–92} where nuclear quantum effects and electronic non-adiabatic effects are both present.

We want to point out that the spin mapping based non-adiabatic Matsubara dynamics method [Eqs. (70) and (73)] is a general theoretical framework, which can be used to derive other state-dependent path-integral approaches, such as the non-adiabatic centroid molecular dynamics⁹³ (through a mean field approximation^{79,94} of the non-adiabatic Matsubara dynamics), taking advantage of the recent progress in the developments of nuclear quantum dynamics based on various approximations of the Matsubara dynamics.^{30,74,79,95–97} We hope that our current work provides a framework for developing accurate quantum dynamics approaches.

ACKNOWLEDGMENTS

This work was supported by the National Science Foundation CAREER Award under Grant No. CHE-1845747. Computing resources were provided by the Center for Integrated Research Computing (CIRC) at the University of Rochester.

AUTHOR DECLARATIONS

Conflict of Interest

The authors have no conflicts to disclose.

Author Contributions

Duncan Bossion: Conceptualization (equal); Data curation (lead); Formal analysis (lead); Investigation (lead); Methodology (lead); Software (lead); Validation (lead); Visualization (lead); Writing – original draft (lead); Writing – review & editing (equal). **Sutirtha N. Chowdhury:** Conceptualization (equal); Formal analysis (equal); Methodology (supporting); Software (supporting); Writing – original draft (supporting). **Pengfei Huo:** Conceptualization (equal); Formal analysis (equal); Investigation (equal); Methodology (equal); Project administration (lead); Resources (lead); Supervision (lead); Writing – original draft (equal); Writing – review & editing (lead).

DATA AVAILABILITY

The data that support the findings of this study are available from the corresponding author upon a reasonable request.

APPENDIX A: ANALYTIC EXPRESSIONS OF THE GENERATORS AND STRUCTURE CONSTANTS IN $\mathfrak{su}(N)$ LIE ALGEBRA

We present the expression of the spin operators \hat{S}_i (equivalent to the generators up to a constant, $\hbar/2$) with $i \in \{1, \dots, N^2 - 1\}$. There are $N(N - 1)/2$ symmetric matrices,

$$\hat{S}_{\alpha_{nm}} = \frac{\hbar}{2} (|m\rangle\langle n| + |n\rangle\langle m|), \quad (\text{A1})$$

$N(N - 1)/2$ antisymmetric matrices,

$$\hat{S}_{\beta_{nm}} = -i\frac{\hbar}{2} (|m\rangle\langle n| - |n\rangle\langle m|), \quad (\text{A2})$$

and $N - 1$ diagonal matrices,

$$\hat{S}_{\gamma_n} = \frac{\hbar}{\sqrt{2n(n-1)}} \left(\sum_{l=1}^{n-1} |l\rangle\langle l| + (1-n)|n\rangle\langle n| \right), \quad (\text{A3})$$

where we introduced the indices α_{nm} related to the symmetric matrices, β_{nm} related to the antisymmetric matrices, and γ_n related to the diagonal matrices as follows:

$$\alpha_{nm} = n^2 + 2(m-n) - 1, \quad (\text{A4a})$$

$$\beta_{nm} = n^2 + 2(m-n), \quad (\text{A4b})$$

$$\gamma_n = n^2 - 1, \quad (\text{A4c})$$

where $1 \leq m < n \leq N$ and $2 \leq n \leq N$, and the generators are ordered according to the conventions.^{56,62}

All the non-zero totally antisymmetric structure constants are expressed as follows:

$$\begin{aligned} f_{\alpha_{nm}\alpha_{kn}\beta_{km}} &= f_{\alpha_{nm}\alpha_{nk}\beta_{km}} = f_{\alpha_{nm}\alpha_{km}\beta_{kn}} = \frac{1}{2}, \\ f_{\beta_{nm}\beta_{km}\beta_{kn}} &= \frac{1}{2}, \\ f_{\alpha_{nm}\beta_{nm}\gamma_m} &= -\sqrt{\frac{m-1}{2m}}, \quad f_{\alpha_{nm}\beta_{nm}\gamma_n} = \sqrt{\frac{n}{2(n-1)}}, \\ f_{\alpha_{nm}\beta_{nm}\gamma_k} &= \sqrt{\frac{1}{2k(k-1)}}, \quad m < k < n. \end{aligned} \quad (\text{A5})$$

All the non-zero totally symmetric structure constants are expressed as follows:

$$\begin{aligned} d_{\alpha_{nm}\alpha_{kn}\alpha_{km}} &= d_{\alpha_{nm}\beta_{kn}\beta_{km}} = d_{\alpha_{nm}\beta_{mk}\beta_{nk}} = \frac{1}{2}, \\ d_{\alpha_{nm}\beta_{nk}\beta_{km}} &= -\frac{1}{2}, \\ d_{\alpha_{nm}\alpha_{nm}\gamma_m} &= d_{\beta_{nm}\beta_{nm}\gamma_m} = -\sqrt{\frac{m-1}{2m}}, \\ d_{\alpha_{nm}\alpha_{nm}\gamma_k} &= d_{\beta_{nm}\beta_{nm}\gamma_k} = \sqrt{\frac{1}{2k(k-1)}}, \quad m < k < n, \\ d_{\alpha_{nm}\alpha_{nm}\gamma_n} &= d_{\beta_{nm}\beta_{nm}\gamma_n} = \frac{2-n}{\sqrt{2n(n-1)}}, \\ d_{\alpha_{nm}\alpha_{nm}\gamma_k} &= d_{\beta_{nm}\beta_{nm}\gamma_k} = \sqrt{\frac{2}{k(k-1)}}, \quad n < k, \\ d_{\gamma_n\gamma_k\gamma_n} &= \sqrt{\frac{2}{n(n-1)}}, \quad k < n, \\ d_{\gamma_n\gamma_n\gamma_n} &= (2-n)\sqrt{\frac{2}{n(n-1)}}. \end{aligned} \quad (\text{A6})$$

Those expressions are valid for any dimension N of the $\mathfrak{su}(N)$ Lie algebra without needing to explicitly compute the commutation and anti-commutation relations. The derivations are provided in the supplementary material of Ref. 51.

APPENDIX B: PHASE SPACE OF THE SPIN-MAPPING VARIABLES

The expansion coefficients of the generalized spin-coherent states in the diabatic basis are^{44,50,59,60}

$$\langle n|\Omega \rangle = \begin{cases} \cos \frac{\theta_1}{2}, & n = 1, \\ \cos \frac{\theta_n}{2} \prod_{l=1}^{n-1} \sin \frac{\theta_l}{2} e^{i\varphi_l}, & 1 < n < N, \\ \prod_{l=1}^{N-1} \sin \frac{\theta_l}{2} e^{i\varphi_l}, & n = N, \end{cases} \quad (\text{B1})$$

with $\{\theta_n\} \in [0, \pi]$ and $\{\varphi_n\} \in [0, 2\pi]$. The $N = 2$ special case of the spin coherent state is expressed in Eq. (D3).

The expression of the differential phase-space volume element $d\Omega$ (which is also referred to as the invariant integration measure on the group), i.e., the Haar measure,⁹⁸ is

$$d\Omega = \frac{N!}{(2\pi)^{N-1}} \prod_{n=1}^{N-1} K_n(\theta_n) d\theta_n d\varphi_n, \quad (\text{B2})$$

where

$$K_n(\theta_n) = \cos \frac{\theta_n}{2} \left(\sin \frac{\theta_n}{2} \right)^{2(N-n)-1}. \quad (\text{B3})$$

When generalizing the above expression for each bead α , they have the same expressions as in Eqs. (B2) and (B3). More specifically,

$$d\Omega^{(\alpha)} = \frac{N!}{(2\pi)^{N-1}} \prod_{n=1}^{N-1} K_n^{(\alpha)} d\theta_n^{(\alpha)} d\varphi_n^{(\alpha)}, \quad (\text{B4a})$$

$$K_n^{(\alpha)} = \cos \frac{\theta_n^{(\alpha)}}{2} \left(\sin \frac{\theta_n^{(\alpha)}}{2} \right)^{2(N-n)-1}, \quad (\text{B4b})$$

and $\langle n|\Omega^{(\alpha)} \rangle$ as a function of $\{\theta_n^{(\alpha)}, \varphi_n^{(\alpha)}\}$ has the same expression in Eq. (B1) for every bead index α .

The expectation values of the spin operators in terms of the angles $\{\theta_i, \varphi_i\}$, $i \in [1, N-1]$ are for the symmetric ones,

$$\begin{aligned} \hbar\Omega_{\alpha_{nm}} &\equiv \langle \Omega | \hat{S}_{\alpha_{nm}} | \Omega \rangle \\ &= \hbar \prod_{j=1}^{m-1} \sin^2 \frac{\theta_j}{2} \cos \frac{\theta_m}{2} \prod_{k=m}^{n-1} \sin \frac{\theta_k}{2} \cos \frac{(1-\delta_{nN})\theta_n}{2} \cos \left(\sum_{l=m}^{n-1} \varphi_l \right), \end{aligned} \quad (\text{B5})$$

with $1 \leq m < n \leq N$. When $m = 1$, $\prod_{j=1}^{m-1} \sin^2 \frac{\theta_j}{2}$ is replaced by 1. Similarly, for the antisymmetric spin operator, we have

$$\begin{aligned} \hbar\Omega_{\beta_{nm}} &\equiv \langle \Omega | \hat{S}_{\beta_{nm}} | \Omega \rangle \\ &= \hbar \prod_{j=1}^{m-1} \sin^2 \frac{\theta_j}{2} \cos \frac{\theta_m}{2} \prod_{k=m}^{n-1} \sin \frac{\theta_k}{2} \cos \frac{(1-\delta_{nN})\theta_n}{2} \sin \left(\sum_{l=m}^{n-1} \varphi_l \right), \end{aligned} \quad (\text{B6})$$

and when $m = 1$, the term $\prod_{j=1}^{m-1} \sin^2 \frac{\theta_j}{2}$ is replaced by 1. For the diagonal spin operators, there is only one index $1 < n \leq N$, and the expression is

$$\begin{aligned} \hbar\Omega_{y_n} &\equiv \langle \Omega | \hat{S}_{y_n} | \Omega \rangle \\ &= \frac{\hbar}{\sqrt{2n(n-1)}} \left(\sum_{j=1}^{n-1} \cos^2 \frac{\theta_j}{2} \prod_{k=1}^{j-1} \sin^2 \frac{\theta_k}{2} + (1-n) \right. \\ &\quad \times \left. \cos^2 \frac{(1-\delta_{nN})\theta_n}{2} \prod_{j=1}^{n-1} \sin^2 \frac{\theta_j}{2} \right), \end{aligned} \quad (\text{B7})$$

where $\prod_{k=1}^{j-1} \sin^2 \frac{\theta_k}{2}$ is replaced by 1 when $n = 2$ (or $j = 1$).

APPENDIX C: DERIVATION OF EQ. (36)

From Eq. (32), we use the properties of the SW transform, as well as perform the Wigner transform on the nuclear DOF, to derive Eq. (36). Here, we provide the details of this derivation. In Eq. (32), we identify

$$\hat{A}_\alpha \equiv e^{-\beta_N \hat{H}} \hat{1}_{R'_\alpha}; \quad \hat{B}_\alpha \equiv e^{\frac{i}{\hbar} \hat{H} t} e^{-\frac{i}{\hbar} \hat{H} t} \hat{1}_{R''_\alpha}, \quad (\text{C1})$$

except for

$$\hat{A}_{N-\alpha} \equiv e^{-\beta_N \hat{H}} \hat{A} \hat{1}'_{R_{N-\alpha}}; \quad \hat{B}_N \equiv e^{\frac{i}{\hbar} \hat{H} t} e^{-\frac{i}{\hbar} \hat{H} t} \hat{B} \hat{1}_{R''_N}. \quad (\text{C2})$$

We further use the property of the SW transform in Eq. (19) to rearrange the integrand in $\int d\{\Omega^{(\alpha)}\}$ as follows:

$$\int d\{\Omega^{(\alpha)}\} [\hat{B}_1 \hat{A}_2 \hat{w}_s^{(2)} \hat{B}_2 \hat{A}_3 \hat{w}_s^{(3)} \hat{B}_3 \cdots \hat{A}_N \hat{w}_s^{(N)} \hat{B}_N \hat{A}_1]_s^{(1)}, \quad (\text{C3})$$

where the competing structure is $\hat{A}_\alpha \hat{w}_s^{(\alpha)} \hat{B}_\alpha$. Using the property in Eq. (19), we can re-express Eq. (C3) as follows:

$$\begin{aligned} &\int d\{\Omega^{(\alpha)}\} [\hat{B}_1]_s^{(1)} [\hat{A}_2 \hat{w}_s^{(2)} \hat{B}_2 \hat{A}_3 \cdots \hat{A}_N \hat{w}_s^{(N)} \hat{B}_N \hat{A}_1]_s^{(1)} \\ &= \int d\{\Omega^{(\alpha)}\} [\hat{B}_1]_s^{(1)} \text{Tr}_e [\hat{A}_2 \hat{w}_s^{(2)} \hat{B}_2 \hat{A}_3 \cdots \hat{A}_N \hat{w}_s^{(N)} \hat{B}_N \hat{A}_1 \hat{w}_s^{(1)}] \\ &= \int d\{\Omega^{(\alpha)}\} [\hat{B}_1]_s^{(1)} \text{Tr}_e [\hat{w}_s^{(2)} \hat{B}_2 \hat{A}_3 \cdots \hat{A}_N \hat{w}_s^{(N)} \hat{B}_N \hat{A}_1 \hat{w}_s^{(1)} \hat{A}_2], \end{aligned} \quad (\text{C4})$$

where from the first to the second line, we used the property in Eq. (18), and for the last equality, we used the property of the trace.

Using $\text{Tr}_e [\hat{w}_s^{(2)} \hat{O}] = [\hat{O}]_s^{(2)}$ [Eq. (10)], we can further express the last line of Eq. (C4) as follows:

$$\begin{aligned} &\int d\{\Omega^{(\alpha)}\} [\hat{B}_1]_s^{(1)} [\hat{B}_2 \hat{A}_3 \cdots \hat{A}_N \hat{w}_s^{(N)} \hat{B}_N \hat{A}_1 \hat{w}_s^{(1)} \hat{A}_2]_s^{(2)} \\ &= \int d\{\Omega^{(\alpha)}\} [\hat{B}_1]_s^{(1)} [\hat{B}_2]_s^{(2)} [\hat{A}_3 \cdots \hat{w}_s^{(N)} \hat{B}_N \hat{A}_1 \hat{w}_s^{(1)} \hat{A}_2]_s^{(2)} \\ &\quad \vdots \\ &= \int d\{\Omega^{(\alpha)}\} \prod_{y=1}^N [\hat{B}_y]_s^{(y)} \cdot \text{Tr}_e \left[\prod_{y=1}^N \hat{A}_y \hat{w}_s^{(y)} \right], \end{aligned} \quad (\text{C5})$$

where from the second line to the last line of the above equation, we have repeated the procedure elaborated in Eq. (C4) for all indices, and the trace in the last line of Eq. (C5) is introduced from $[\dots]_s^{(N)}$.

Using Eq. (C5), we can rewrite Eq. (32) as follows:

$$\begin{aligned} C_{AB}^{[N]}(t) &= \frac{1}{Z} \int d\{R'_\alpha\} \int d\{R''_\alpha\} \int d\{\Omega^{(\alpha)}\} \frac{1}{N} \\ &\times \sum_{\alpha=1}^N \text{Tr}_e \left[\prod_{y=\alpha}^N \langle R''_{y-1} | e^{-\beta_N \hat{H}} | R'_y \rangle \hat{w}_s^{(y)} \langle R''_{\alpha-1} | e^{-\beta_N \hat{H}} A | R'_\alpha \rangle \hat{w}_s^{(\alpha)} \right] \\ &\times \prod_{y \neq N} \left[\langle R''_y | e^{\frac{i}{\hbar} \hat{H} t} e^{-\frac{i}{\hbar} \hat{H} t} | R'_y \rangle \right]_s^{(y)} \left[\langle R''_N | e^{\frac{i}{\hbar} \hat{H} t} \hat{B} e^{-\frac{i}{\hbar} \hat{H} t} | R'_N \rangle \right]_s^{(N)}. \end{aligned} \quad (\text{C6})$$

Further using the cyclic-symmetric property to write the operator \hat{B} into a bead-averaged fashion (i.e., placing \hat{B} in different blocks), we obtain Eq. (36) of the main text.

APPENDIX D: SM-NRPMD FOR TWO-STATE SYSTEMS

We consider a two-level system $\hat{H} = \frac{\hat{p}^2}{2M} \hat{I} + U_0(\hat{R}) \hat{I} + \hat{V}_e(\hat{R})$, where \hat{I} is the 2×2 identity matrix and

$$\hat{V}_e(\hat{R}) = \begin{pmatrix} V_{11}(\hat{R}) & V_{12}(\hat{R}) \\ V_{21}(\hat{R}) & V_{22}(\hat{R}) \end{pmatrix}. \quad (\text{D1})$$

For this special case, $f_{ijk} = \varepsilon_{ijk}$ and $d_{ijk} = 0$, and all the equations in the main text remain general. Nevertheless, it will be beneficial to explicitly give several key equations under this special limit, whereas more detailed discussion on $SU(2)$ can be found in the previous work on spin-LSC⁴³ as well as in spin-mapping non-adiabatic RPMD (SM-NRPMD).⁵²

Using the $SU(2)$ representation, one can express the original two-states Hamiltonian as follows:⁴³

$$\hat{H} = \mathcal{H}_0 \hat{I} + \frac{1}{\hbar} \mathbf{H} \cdot \hat{\mathbf{S}} = \mathcal{H}_0 \hat{I} + \frac{1}{\hbar} (\mathcal{H}_x \cdot \hat{S}_x + \mathcal{H}_y \cdot \hat{S}_y + \mathcal{H}_z \cdot \hat{S}_z), \quad (\text{D2})$$

where $\hat{S}_i = \frac{\hbar}{2} \hat{\sigma}_i$ (for $i \in \{x, y, z\}$) with $\hat{\sigma}_i$ as the Pauli matrices and $\mathcal{H}_0 = \frac{\hat{p}^2}{2m} + U_0(\hat{R}) + \frac{1}{2}(V_{11}(\hat{R}) + V_{22}(\hat{R}))$, $\mathcal{H}_x = 2\text{Re}(V_{12}(\hat{R}))$, $\mathcal{H}_y = 2\text{Im}(V_{12}(\hat{R}))$, $\mathcal{H}_z = V_{11}(\hat{R}) - V_{22}(\hat{R})$, which is the $N = 2$ limit of Eq. (6).

For $N = 2$, the spin coherent state in Eq. (7) is expressed as

$$|\Omega\rangle = \cos \frac{\theta_1}{2} |1\rangle + \sin \frac{\theta_1}{2} e^{i\varphi_1} |2\rangle, \quad (\text{D3})$$

and the expectation value of the spin operator is

$$\hbar\Omega_i^{(\alpha)}(\Omega) = \langle \Omega^{(\alpha)} | \hat{S}_i | \Omega^{(\alpha)} \rangle, \quad i \in \{x, y, z\}, \quad (\text{D4})$$

where $\Omega_x = \frac{1}{2} \sin \theta \cos \varphi$, $\Omega_y = \frac{1}{2} \sin \theta \sin \varphi$, and $\Omega_z = \frac{1}{2} \cos \theta$ as the special case of Eqs. (B5)–(B7), and Eq. (B2) becomes $d\Omega = \frac{1}{2\pi} \sin \theta d\theta d\varphi$.

The derivation procedure of the Kubo-transformed TCF and exact Liouvillian are same as outlined in the main text. All the approximations made to obtain the Matsubara and SM-NRPMD expressions of the TCFs are identical. For the $N = 2$ special case (when \hat{V} is purely real), the SM-NRPMD Hamiltonian is

$$\begin{aligned} \mathcal{H}_{\mathcal{N}} &= H_{\text{rp}}^{[\mathcal{N}]} + r_s \sum_{\alpha=1}^{\mathcal{N}} \mathcal{H}^{(\alpha)} \cdot \Omega^{(\alpha)} \\ &= \sum_{\alpha=1}^{\mathcal{N}} \left[\mathcal{H}_0(R_\alpha, P_\alpha) + \frac{m}{2\beta_{\mathcal{N}}^2 \hbar^2} (R_\alpha - R_{\alpha-1})^2 + \left(\frac{1}{2} + r_s \cos \theta \right) \right. \\ &\quad \cdot V_{11}(R_\alpha) + \left(\frac{1}{2} - r_s \cos \theta \right) \\ &\quad \cdot V_{22}(R_\alpha) + 2r_s \sin \theta \cos \varphi \cdot V_{12}(R_\alpha) \right], \end{aligned} \quad (\text{D5})$$

with $H_{\text{rp}}^{[\mathcal{N}]}$ defined in the main text and $\mathcal{H}^{(\alpha)} = \{\mathcal{H}_x(R_\alpha), \mathcal{H}_y(R_\alpha), \mathcal{H}_z(R_\alpha)\}$.

The electronic EOMs under the linearization approximation can be expressed as

$$\dot{\Omega}^{(\alpha)} = \frac{1}{\hbar} \sum_{j,k=1}^3 \varepsilon_{ijk} \mathcal{H}_j(R_\alpha) \Omega_k^{(\alpha)} = \frac{1}{\hbar} \mathbf{H}(R_\alpha) \times \Omega^{(\alpha)}, \quad (\text{D6})$$

where \times denotes the cross product of two vectors. This equation is the special case of Eq. (90c) for $N = 2$. Here, ε_{ijk} is the Levi-Civita symbol, which is the totally antisymmetric structure constant of the $\mathfrak{su}(2)$ Lie algebra. One can also express Eq. (D6) in terms of the MMST mapping variables, which is Eq. (98) with $N = 2$. In addition, Eq. (D6) also has a rather simple expression using the Euler angles $\{\theta^{(\alpha)}, \varphi^{(\alpha)}\}$,

$$\begin{aligned} \dot{\theta}^{(\alpha)} &= \frac{1}{\hbar} \left(-\mathcal{H}_x \sin \varphi^{(\alpha)} + \mathcal{H}_y \cos \varphi^{(\alpha)} \right), \\ \dot{\varphi}^{(\alpha)} &= \frac{1}{\hbar} \left(\mathcal{H}_z - \mathcal{H}_x \frac{\cos \varphi^{(\alpha)}}{\tan \theta^{(\alpha)}} - \mathcal{H}_y \frac{\sin \varphi^{(\alpha)}}{\tan \theta^{(\alpha)}} \right), \end{aligned} \quad (\text{D7})$$

whereas the equivalent equations for $N > 2$ are rather complicated, with details provided in Appendix E of Ref. 51.

In the two-state case, the initial electronic phase $\hat{\Gamma}_{\tilde{s}}$ [Eq. (71)] can be analytically expressed [thanks to the special property of the $SU(2)$ Lie group] as⁵²

$$\begin{aligned} \hat{\Gamma}_{\tilde{s}} &= \prod_{\alpha}^{\mathcal{N}} e^{-\beta_{\mathcal{N}} \frac{1}{\hbar} \sum_k \mathcal{H}_k(R_\alpha) \cdot \hat{\mathcal{S}}_k} \cdot \hat{w}_{\tilde{s}}^{(\alpha)} \\ &= \prod_{\alpha}^{\mathcal{N}} \left[\left(\frac{1}{2} \cosh \eta - r_s \frac{\mathcal{H}^{(\alpha)}}{|\mathcal{H}^{(\alpha)}|} \cdot \Omega^{(\alpha)} \sinh \eta \right) \cdot \hat{\mathcal{I}} + \left(r_s \Omega^{(\alpha)} \cosh \eta \right. \right. \\ &\quad \left. \left. - \left(\frac{1}{2} \frac{\mathcal{H}^{(\alpha)}}{|\mathcal{H}^{(\alpha)}|} + ir_s \frac{\mathcal{H}^{(\alpha)}}{|\mathcal{H}^{(\alpha)}|} \times \Omega^{(\alpha)} \right) \sinh \eta \right) \cdot \frac{2}{\hbar} \hat{\mathcal{S}} \right], \end{aligned} \quad (\text{D8})$$

where for convenience we defined

$$\begin{aligned} \mathcal{H}^{(\alpha)} \cdot \Omega^{(\alpha)} &\equiv \sum_{k=1}^3 \mathcal{H}_k(R_\alpha) \cdot \Omega_k^{(\alpha)}, \\ \left[\mathcal{H}^{(\alpha)} \times \Omega^{(\alpha)} \right]_i &\equiv \sum_{i,j,k=1}^3 f_{ijk} \mathcal{H}_j(R_\alpha) \cdot \Omega_k^{(\alpha)}, \\ |\mathcal{H}^{(\alpha)}| &\equiv \sqrt{\sum_{k=1}^3 \mathcal{H}_k^2(R_\alpha)}, \quad \eta \equiv \frac{\beta_{\mathcal{N}} |\mathcal{H}^{(\alpha)}|}{2}. \end{aligned} \quad (\text{D9})$$

The details of the derivation can be found in Appendix D of Ref. 52. The advantage of having this analytic expression is that it

avoids the numerical cost of evaluating the exponential by diagonalizing it. Unfortunately, we did not obtain the analytic expression for the general N -level case due to the totally symmetric structure constants d_{ijk} , which do not cancel beyond $N = 2$, making the exponential not exactly factorizable in terms of hyperbolic cosines and sines. That said, there might still exist alternative ways to evaluate it to get a closed analytic expression for $\hat{\Gamma}_{\tilde{s}}$ [Eq. (71)] for a general N -state system.

APPENDIX E: NON-EQUILIBRIUM DYNAMICS

In our previous work, we have justified that NRPMD is also capable of accurately describing the non-equilibrium TCF. Here, we carry the same procedure and show that the SM-NRPMD is also capable to describe the non-equilibrium TCF. For a given photo-induced process, we are often interested in the reduced density matrix dynamics upon an initial excitation of the molecular system. The reduced density matrix element can be expressed as

$$\rho_{nm}(t) = \text{Tr} \left[\hat{\rho}(0) e^{\frac{i}{\hbar} \hat{H} t} |n\rangle \langle m| e^{-\frac{i}{\hbar} \hat{H} t} \right], \quad (\text{E1})$$

where the initial density operator $\hat{\rho}(0) = |a\rangle \langle a| \otimes \frac{1}{Z} e^{-\beta \hat{H}_g}$ is a tensor product of the electronic and nuclear DOFs, with $Z = \text{Tr}[e^{-\beta \hat{H}_g}]$, and \hat{H}_g is the ground state Hamiltonian,

$$\hat{H}_g = \hat{T}_R + U_g(\hat{R}), \quad (\text{E2})$$

with the ground state potential $U_g(\hat{R})$ associated with the ground electronic state $|g\rangle$.

The initial density $\hat{\rho}(0)$ evolves under the influence of the total Hamiltonian \hat{H} of the system. The reduced density matrix elements can be equivalently expressed as a TCF,

$$\rho_{nm}(t) = C_{AB}(t) = \frac{1}{Z} \text{Tr} \left[e^{-\beta \hat{H}_g} \hat{A} e^{\frac{i}{\hbar} \hat{H} t} \hat{B} e^{-\frac{i}{\hbar} \hat{H} t} \right], \quad (\text{E3})$$

where $\hat{A} = |a\rangle \langle a|$ is the initially occupied electronic state and $\hat{B} = |n\rangle \langle m|$. Because \hat{A} and \hat{H}_g commute, we have

$$\begin{aligned} C_{AB}^{[\mathcal{N}]}(t) &= \frac{1}{Z\beta} \int_0^\beta d\lambda \text{Tr} \left[e^{-(\beta-\lambda)\hat{H}_g} \hat{A} e^{-\lambda \hat{H}_g} \hat{B}(t) \right] \\ &= \frac{\int_0^\beta d\lambda}{\beta} \cdot \frac{1}{Z} \text{Tr} \left[e^{-\beta \hat{H}_g} \hat{A} \hat{B}(t) \right] = C_{AB}(t). \end{aligned} \quad (\text{E4})$$

Hence, one can rewrite the reduced density matrix elements $\rho_{nm}(t)$ into the Kubo-transformed time-correlation function $C_{AB}^{[\mathcal{N}]}(t)$. This Kubo-transformed TCF is *not* an equilibrium correlation function. Nevertheless, the Kubo-transformed structure allows us to express it as the discrete version of the time-correlation function. Following the same derivation outlined in the main text, we can obtain the out-of-equilibrium SM-NRPMD TCF,

$$\begin{aligned} \rho_{nm}(t) &= \frac{1}{Z(2\pi\hbar)^{\mathcal{N}}} \int \{dR\} \int \{dP\} \int \{d\Omega\} e^{-\beta_{\mathcal{N}} H_{\text{rp}}^{[\mathcal{N}]}} \\ &\quad \times \text{Tr} \left[\prod_{\alpha=1}^{\mathcal{N}} \hat{w}_{\tilde{s}}^{(\alpha)} |a\rangle \langle a| \right] e^{\mathcal{L}_{\text{rp}}^{[\mathcal{N}]} t} [|n\rangle \langle m|]_s, \end{aligned} \quad (\text{E5})$$

where $H_{\text{rp}}^{[\mathcal{N}]}$ is expressed as

$$H_{\text{rp}}^{[\mathcal{N}]} = \sum_{\alpha=1}^{\mathcal{N}} \left[\mathcal{H}_g(R_\alpha, P_\alpha) + \frac{m}{2\beta_{\mathcal{N}} \hbar^2} (R_\alpha - R_{\alpha-1})^2 \right], \quad (\text{E6})$$

and the bead-averaged estimator $\langle |n\rangle \langle m| \rangle_s$ is expressed in Eq. (106). The initial electronic phase $\text{Tr}_e \left[\prod_{\alpha=1}^{\mathcal{N}} \hat{w}_{\text{s}}^{(\alpha)} |a\rangle \langle a| \right]$ is expressed as

$$\text{Tr}_e \left[\prod_{\alpha=1}^{\mathcal{N}} \hat{w}_{\text{s}}^{(\alpha)} |a\rangle \langle a| \right] = \frac{1}{\mathcal{N}} \sum_{\alpha=1}^{\mathcal{N}} \text{Tr}_e \left[\prod_{\gamma \leq \alpha}^{\mathcal{N}} \hat{w}_{\text{s}}^{(\gamma)} |a\rangle \langle a| \prod_{\gamma > \alpha}^{\mathcal{N}} \hat{w}_{\text{s}}^{(\gamma)} \right]. \quad (\text{E7})$$

Furthermore, the Liouvillian $\mathcal{L}_{\text{rp}}^{[\mathcal{N}]}$ corresponds to the EOM in Eq. (98).

APPENDIX F: MMST-BASED NRPMD APPROACH AND THE EXACT SIMULATION

The original MMST-based NRPMD approach to compute position auto-correlation function was proposed as¹¹

$$C_{RR}^{[\mathcal{N}]}(t) = \frac{1}{Z_{\mathcal{N}}} \int d\{R_\alpha\} \int d\{P_\alpha\} \int d\{\mathbf{q}^{(\alpha)}\} \int d\{\mathbf{p}^{(\alpha)}\} \times e^{-\beta_{\mathcal{N}} H_{\text{rp}}^{[\mathcal{N}]} t} \phi e^{-\frac{G_{\mathcal{N}}}{\hbar} t} \text{Tr}_e [\hat{\Gamma}] \tilde{R} e^{\mathcal{L}_{\text{rp}}^{[\mathcal{N}]} t} \tilde{R}(t), \quad (\text{F1})$$

where $d\{\mathbf{q}^{(\alpha)}\} = \prod_{\alpha=1}^{\mathcal{N}} d\mathbf{q}^{(\alpha)}$, $d\{\mathbf{p}^{(\alpha)}\} = \prod_{\alpha=1}^{\mathcal{N}} d\mathbf{p}^{(\alpha)}$, and $\mathbf{q}^{(\alpha)} = \{q_1^{(\alpha)}, \dots, q_N^{(\alpha)}\}$, $\mathbf{p}^{(\alpha)} = \{p_1^{(\alpha)}, \dots, p_N^{(\alpha)}\}$. Furthermore, $\phi = \left(\frac{4}{\pi N}\right)^{\mathcal{N}}$, $G_{\mathcal{N}} = \sum_{\alpha=1}^{\mathcal{N}} ([\mathbf{q}^{(\alpha)}]^T \mathbf{q}^{(\alpha)} + [\mathbf{p}^{(\alpha)}]^T \mathbf{p}^{(\alpha)})$, and $\tilde{R} = \frac{1}{\mathcal{N}} \sum_{\alpha=1}^{\mathcal{N}} R_\alpha$ is the bead average position. In addition, $\hat{\Gamma}$ is expressed as¹¹

$$\hat{\Gamma} = \prod_{\alpha=1}^{\mathcal{N}} \mathcal{M}(R_\alpha) \mathbf{q}^{(\alpha)} [\mathbf{q}^{(\alpha)}]^T \mathcal{M}(R_\alpha) \mathbf{p}^{(\alpha)} [\mathbf{p}^{(\alpha)}]^T, \quad (\text{F2})$$

where $\mathcal{M}_{nm}(R_\alpha) = \langle n | e^{-\frac{1}{2} \beta_{\mathcal{N}} \hat{V}_e(R_\alpha)} | m \rangle$ and $[\mathbf{q}^{(\alpha)}]^T$ represents the transpose of the $\mathbf{q}^{(\alpha)}$ row matrix. The Liouvillian $\mathcal{L}_{\text{rp}}^{[\mathcal{N}]}$ (in terms of the MMST mapping variables) is identical to the corresponding one in SM-NRPMD, both corresponding to the EOMs in Eq. (98).

To compute a population TCF, the NRPMD approach uses¹¹

$$C_{mn}^{[\mathcal{N}]}(t) = \frac{1}{Z_{\mathcal{N}}} \int d\{R_\alpha\} \int d\{P_\alpha\} \int d\{\mathbf{q}_\alpha\} \int d\{\mathbf{p}_\alpha\} \times e^{-\beta_{\mathcal{N}} H_{\text{rp}}^{[\mathcal{N}]} t} \phi e^{-\frac{G_{\mathcal{N}}}{\hbar} t} \text{Tr}_e [\hat{\Gamma} \hat{A}] e^{\mathcal{L}_{\text{rp}}^{[\mathcal{N}]} t} \tilde{B}_n, \quad (\text{F3})$$

where \tilde{B}_n is the bead average projection operator expressed in Eq. (106), with $\gamma = 1$ corresponding to the ZPE parameter in the MMST mapping theory,^{28,29} and $\text{Tr}_e [\hat{\Gamma} \hat{A}]$ is computed as

$$\text{Tr}_e [\hat{\Gamma} \hat{A}] = \frac{1}{\mathcal{N}} \sum_{\alpha} \text{Tr}_e \left[\prod_{\gamma \leq \alpha}^{\mathcal{N}} \mathcal{M}(R_\gamma) \mathbf{q}^{(\gamma)} [\mathbf{q}^{(\gamma)}]^T \mathcal{M}(R_\gamma) \mathbf{p}^{(\gamma)} [\mathbf{p}^{(\gamma)}]^T \hat{A} \times \prod_{\gamma > \alpha}^{\mathcal{N}} \mathcal{M}(R_\gamma) \mathbf{q}^{(\gamma)} [\mathbf{q}^{(\gamma)}]^T \mathcal{M}(R_\gamma) \mathbf{p}^{(\gamma)} [\mathbf{p}^{(\gamma)}]^T \right]. \quad (\text{F4})$$

Thus, the dynamics between the SM version and the MMST version of NRPMD are identical, and the difference between them comes

from the initial distributions of the mapping variables and the choice and justification of the γ value (so-called ZPE parameter).

Note that this is the original version of the MMST-based NRPMD approach,^{11,12} which has a different sampling than the NRPMD method derived from Kubo-transformed TCF in Ref. 25. In fact, when derived from the Matsubara approximation, the distribution is identical to the MV-RPMD method.¹⁴ Due to the severe sign problem encountered for the three-state system, we could not converge our results with the MV-RPMD sampling approach. Nevertheless, the original MMST-based NRPMD method gives results very similar to the NRPMD method derived in Ref. 25; hence, we just use the original version of the NRPMD algorithm. The numerical details are referred back to the original NRPMD papers in Refs. 11 and 12.

The exact results are obtained by explicitly computing the Kubo-transformed TCF as follows:

$$C_{AB}^K(t) = \frac{1}{Z\mathcal{N}} \sum_{\alpha=1}^{\mathcal{N}} \text{Tr} \left[e^{-\beta_{\mathcal{N}}(\mathcal{N}-\alpha)\hat{H}} \hat{A} e^{-\beta_{\mathcal{N}}\alpha\hat{H}} e^{\frac{i}{\hbar}\hat{H}t} \hat{B} e^{-\frac{i}{\hbar}\hat{H}t} \right], \quad (\text{F5})$$

where the trace is for both electronic and nuclear DOFs. To evaluate the trace, we explicitly calculate the eigenstate of \hat{H} .

The full Hilbert space of the entire system is represented with a basis composed by a tensor product of the electronic subspace $\{|n\rangle\}$ and the Fock states $\{|\chi_a\rangle\}$ of the nuclear DOFs as follows:

$$|n\rangle \otimes |\chi_a\rangle \equiv |n, \chi_a\rangle, \quad (\text{F6})$$

where $|n\rangle$ is the electronic diabatic states and $|\chi_a\rangle$ is the eigenstate of $\frac{p^2}{2m} + \frac{1}{2}m\omega\hat{R}^2$. We solve the eigenvalue problem of the total Hamiltonian as follows:

$$\hat{H}|\Psi_v\rangle = E_v|\Psi_v\rangle, \quad (\text{F7})$$

where $|\Psi_v\rangle = \sum_{n,a} c_{n,a}^v |n, \chi_a\rangle$ is the eigenstate of the entire system (including both electronic and nuclear DOFs) and $c_{n,a}^v = \langle n, \chi_a | \Psi_v \rangle$ is the expansion coefficient. Both E_v and $c_{n,a}^v$ can be directly obtained from diagonalizing the matrix of \hat{H} with the matrix elements $\langle \chi_b, m | \hat{H} | n, \chi_a \rangle$. Evaluating $\text{Tr}[\hat{O}]$ in Eq. (F5) as $\sum_v \langle \Psi_v | \hat{O} | \Psi_v \rangle$, the Kubo-transformed TCF is expressed as

$$C_{AB}^K(t) = \frac{1}{Z\mathcal{N}} \sum_{\alpha=1}^{\mathcal{N}} \sum_{v,\mu} e^{-\beta_{\mathcal{N}}(\mathcal{N}-\alpha)E_v} [\hat{A}]_{v\mu} e^{-\beta_{\mathcal{N}}\alpha E_\mu} e^{\frac{i}{\hbar}E_\mu t} [\hat{B}]_{\mu\nu} e^{-\frac{i}{\hbar}E_\nu t}, \quad (\text{F8})$$

where the matrix $[\hat{A}]_{v\mu}$ is

$$[\hat{A}]_{v\mu} = \langle \Psi_v | \hat{A} | \Psi_\mu \rangle = \sum_{n,a} \sum_{m,b} (c_{n,a}^v)^* \langle \chi_a, n | \hat{A} | m, \chi_b \rangle c_{m,b}^\mu \quad (\text{F9})$$

and similarly for $[\hat{B}]_{\mu\nu} = \langle \Psi_\mu | \hat{B} | \Psi_v \rangle$. When $\hat{A} = \hat{R}$, $[\hat{A}]_{v\mu} = \sqrt{\frac{\hbar}{m\omega}} \sqrt{\frac{a+1}{2}} \delta_{m,n+1}$, and $\hat{A} = |m\rangle \langle m|$, $[\hat{A}]_{v\mu} = \delta_{mn} \delta_{ab}$. For the partition function in Eq. (F8), one can evaluate it exactly as

$$\mathcal{Z} = \text{Tr}[e^{-\beta\hat{H}}] = \sum_v \langle \Psi_v | e^{-\beta\hat{H}} | \Psi_v \rangle = \sum_v e^{-\beta E_v}.$$

For the model systems studied here, solving the eigenvalue problem in Eq. (F7) requires about 50 Fock states $\{|\chi_a\rangle\}$ to represent the nuclear operators, and the TCF in Eq. (F8) converges with $\mathcal{N} = 6$.

REFERENCES

- ¹J. C. Tully, *J. Chem. Phys.* **137**, 22A301 (2012).
- ²R. A. Marcus and N. Sutin, *Biochim. Biophys. Acta, Bioenerg.* **811**, 265 (1985).
- ³H. B. Gray and J. R. Winkler, *Annu. Rev. Biochem.* **65**, 537 (1996).
- ⁴S. Y. Reece and D. G. Nocera, *Annu. Rev. Biochem.* **78**, 673 (2009).
- ⁵I. R. Craig and D. E. Manolopoulos, *J. Chem. Phys.* **121**, 3368 (2004).
- ⁶I. R. Craig and D. E. Manolopoulos, *J. Chem. Phys.* **123**, 034102 (2005).
- ⁷I. R. Craig and D. E. Manolopoulos, *J. Chem. Phys.* **122**, 084106 (2005).
- ⁸Y. V. Suleimanov, J. W. Allen, and W. H. Green, *Comput. Phys. Commun.* **184**, 833 (2013).
- ⁹Y. V. Suleimanov, R. P. de Tudela, P. G. Jambrina, J. F. Castillo, V. Sáez-Rábanos, D. E. Manolopoulos, and F. J. Aoiz, *Phys. Chem. Chem. Phys.* **15**, 3655 (2013).
- ¹⁰T. J. H. Hele, “An electronically non-adiabatic generalization of ring polymer molecular dynamics,” M.S. thesis, Oxford University, 2011; arXiv:1308.3950 [physics.chem-ph] (2013).
- ¹¹J. O. Richardson and M. Thoss, *J. Chem. Phys.* **139**, 031102 (2013).
- ¹²J. O. Richardson, P. Meyer, M.-O. Pleinert, and M. Thoss, *Chem. Phys.* **482**, 124 (2017).
- ¹³S. N. Chowdhury and P. Huo, *J. Chem. Phys.* **150**, 244102 (2019).
- ¹⁴N. Ananth, *J. Chem. Phys.* **139**, 124102 (2013).
- ¹⁵J. R. Duke and N. Ananth, *J. Phys. Chem. Lett.* **6**, 4219 (2015).
- ¹⁶S. Pierre, J. R. Duke, T. J. H. Hele, and N. Ananth, *J. Chem. Phys.* **147**, 234103 (2017).
- ¹⁷T. Yoshikawa and T. Takayanagi, *Chem. Phys. Lett.* **564**, 1 (2013).
- ¹⁸A. R. Menzeliev, F. Bell, and T. F. Miller, *J. Chem. Phys.* **140**, 064103 (2014).
- ¹⁹J. S. Kretchmer and T. F. Miller III, *Faraday Discuss.* **195**, 191 (2016).
- ²⁰S. N. Chowdhury and P. Huo, *J. Chem. Phys.* **147**, 214109 (2017).
- ²¹P. Shushkov, R. Li, and J. C. Tully, *J. Chem. Phys.* **137**, 22A549 (2012).
- ²²F. A. Shakib and P. Huo, *J. Phys. Chem. Lett.* **8**, 3073 (2017).
- ²³X. Tao, P. Shushkov, and T. F. Miller, *J. Chem. Phys.* **148**, 102327 (2018).
- ²⁴X. Tao, P. Shushkov, and T. F. Miller, *J. Phys. Chem. A* **123**, 3013 (2019).
- ²⁵S. N. Chowdhury and P. Huo, *J. Chem. Phys.* **154**, 124124 (2021).
- ²⁶S. N. Chowdhury, A. Mandal, and P. Huo, *J. Chem. Phys.* **154**, 044109 (2021).
- ²⁷H. D. Meyer and W. H. Miller, *J. Chem. Phys.* **70**, 3214 (1979).
- ²⁸G. Stock and M. Thoss, *Phys. Rev. Lett.* **78**, 578 (1997).
- ²⁹M. Thoss and G. Stock, *Phys. Rev. A* **59**, 64 (1999).
- ³⁰T. J. H. Hele, M. J. Willatt, A. Muolo, and S. C. Althorpe, *J. Chem. Phys.* **142**, 134103 (2015).
- ³¹S. C. Althorpe, N. Ananth, G. Angulo, R. D. Astumian, V. Beniwal, J. Blumberger, P. G. Bolhuis, B. Ensing, D. R. Glowacki, S. Habershon, S. Hammes-Schiffer, T. J. H. Hele, N. Makri, D. E. Manolopoulos, L. K. McKemmish, T. F. Miller III, W. H. Miller, A. J. Mulholland, T. Nekipelova, E. Pollak, J. O. Richardson, M. Richter, P. Roy Chowdhury, D. Shalashilin, and R. Szabla, *Faraday Discuss.* **195**, 311 (2016).
- ³²X. Sun and W. H. Miller, *J. Chem. Phys.* **106**, 916 (1997).
- ³³E. A. Coronado, J. Xing, and W. H. Miller, *Chem. Phys. Lett.* **349**, 521 (2001).
- ³⁴S. Bonella and D. F. Coker, *J. Chem. Phys.* **114**, 7778 (2001).
- ³⁵H. Kim, A. Nassimi, and R. Kapral, *J. Chem. Phys.* **129**, 084102 (2008).
- ³⁶P. Huo and D. F. Coker, *J. Chem. Phys.* **135**, 201101 (2011).
- ³⁷P. Huo and D. F. Coker, *J. Chem. Phys.* **137**, 22A535 (2012).
- ³⁸W. H. Miller and S. J. Cotton, *Faraday Discuss.* **195**, 9 (2016).
- ³⁹N. Ananth and T. F. Miller, *J. Chem. Phys.* **133**, 234103 (2010).
- ⁴⁰A. Kelly, R. van Zon, J. Schofield, and R. Kapral, *J. Chem. Phys.* **136**, 084101 (2012).
- ⁴¹M. A. C. Saller, A. Kelly, and J. O. Richardson, *J. Chem. Phys.* **150**, 071101 (2019).
- ⁴²S. J. Cotton and W. H. Miller, *J. Chem. Phys.* **139**, 234112 (2013).
- ⁴³J. E. Runeson and J. O. Richardson, *J. Chem. Phys.* **151**, 044119 (2019).
- ⁴⁴J. E. Runeson and J. O. Richardson, *J. Chem. Phys.* **152**, 084110 (2020).
- ⁴⁵R. L. Stratonovich, *Sov. Phys. JETP* **4**, 891 (1957).
- ⁴⁶J. C. Várilly and J. Gracia-Bondía, *Ann. Phys.* **190**, 107 (1989).
- ⁴⁷C. Brif and A. Mann, *Phys. Rev. A* **59**, 971 (1999).
- ⁴⁸A. B. Klimov and S. M. Chumakov, *A Group-Theoretical Approach to Quantum Optics: Models of Atom-Field Interactions* (John Wiley and Sons, 2009).
- ⁴⁹J. M. Radcliffe, *J. Phys. A: Gen. Phys.* **4**, 313 (1971).
- ⁵⁰K. Nemoto, *J. Phys. A: Math. Gen.* **33**, 3493 (2000).
- ⁵¹D. Bossion, W. Ying, S. N. Chowdhury, and P. Huo, *J. Chem. Phys.* **157**, 084105 (2022).
- ⁵²D. Bossion, S. N. Chowdhury, and P. Huo, *J. Chem. Phys.* **154**, 184106 (2021).
- ⁵³H. Georgi, *Lie Algebras in Particle Physics: From Isospin to Unified Theories* (CRC Press, 2000).
- ⁵⁴B. C. Hall, *GTM222: Lie Groups, Lie Algebras, and Representations: An Elementary Introduction*, 2nd ed. (Springer, Cham, Switzerland, 2015).
- ⁵⁵M. Gell-Mann, *Phys. Rev.* **125**, 1067 (1962).
- ⁵⁶W. Pfeifer, *The Lie Algebras SU(N): An Introduction* (Springer, 2003).
- ⁵⁷T. Tilma and K. Nemoto, *J. Phys. A: Math. Theor.* **45**, 015302 (2011).
- ⁵⁸F. T. Hioe and J. H. Eberly, *Phys. Rev. Lett.* **47**, 838 (1981).
- ⁵⁹T. Tilma and E. C. G. Sudarshan, *J. Phys. A: Math. Gen.* **35**, 10467 (2002).
- ⁶⁰T. Tilma and E. C. G. Sudarshan, *J. Geom. Phys.* **52**, 263 (2004).
- ⁶¹G. Kimura, *Phys. Lett. A* **314**, 339 (2003).
- ⁶²R. A. Bertlmann and P. Krammer, *J. Phys. A: Math. Theor.* **41**, 235303 (2008).
- ⁶³C. Brif and A. Mann, *J. Phys. A: Math. Gen.* **31**, L9 (1998).
- ⁶⁴F. Bloch, *Phys. Rev.* **70**, 460 (1946).
- ⁶⁵R. K. Wangsness and F. Bloch, *Phys. Rev.* **89**, 728 (1953).
- ⁶⁶I. I. Rabi, N. F. Ramsey, and J. Schwinger, *Rev. Mod. Phys.* **26**, 167 (1954).
- ⁶⁷E. Wigner, *Phys. Rev.* **40**, 749 (1932).
- ⁶⁸H. J. Groenewold, *Physica* **12**, 405 (1946).
- ⁶⁹K. Ímre, E. Özizmir, M. Rosenbaum, and P. F. Zweifel, *J. Math. Phys.* **8**, 1097 (1967).
- ⁷⁰M. Hillery, R. F. O’Connell, M. O. Scully, and E. P. Wigner, *Phys. Rep.* **106**, 121 (1984).
- ⁷¹Q. Shi and E. Geva, *J. Chem. Phys.* **118**, 8173 (2003).
- ⁷²T. J. H. Hele and N. Ananth, *Faraday Discuss.* **195**, 269 (2016).
- ⁷³J. A. Poulsen, G. Nyman, and P. J. Rossky, *J. Chem. Phys.* **119**, 12179 (2003).
- ⁷⁴M. J. Willatt, “Matsubara dynamics and its practical implementations,” Ph.D. thesis, University of Cambridge, 2017.
- ⁷⁵D. L. Freeman and J. D. Doll, *J. Chem. Phys.* **80**, 5709 (1984).
- ⁷⁶C. Chakravarty, *Int. Rev. Phys. Chem.* **16**, 421 (1997).
- ⁷⁷C. Chakravarty, M. C. Gordillo, and D. M. Ceperley, *J. Chem. Phys.* **109**, 2123 (1998).
- ⁷⁸D. M. Ceperley, *Rev. Mod. Phys.* **67**, 279 (1995).
- ⁷⁹T. J. H. Hele, M. J. Willatt, A. Muolo, and S. C. Althorpe, *J. Chem. Phys.* **142**, 191101 (2015).
- ⁸⁰S. Habershon, D. E. Manolopoulos, T. E. Markland, and T. F. Miller, *Annu. Rev. Phys. Chem.* **64**, 387 (2013).
- ⁸¹J. E. Runeson and J. O. Richardson, *Phys. Rev. Lett.* **127**, 250403 (2021).
- ⁸²R. P. Feynman, F. L. Vernon, and R. W. Hellwarth, *J. Appl. Phys.* **28**, 49 (1957).
- ⁸³A. Heslot, *Phys. Rev. D* **31**, 1341 (1985).
- ⁸⁴N. Metropolis, A. W. Rosenbluth, M. N. Rosenbluth, A. H. Teller, and E. Teller, *J. Chem. Phys.* **21**, 1087 (1953).
- ⁸⁵W. K. Hastings, *Biometrika* **57**, 97 (1970).
- ⁸⁶M. Ceriotti, M. Parrinello, T. E. Markland, and D. E. Manolopoulos, *J. Chem. Phys.* **133**, 124104 (2010).
- ⁸⁷M. S. Church, T. J. H. Hele, G. S. Ezra, and N. Ananth, *J. Chem. Phys.* **148**, 102326 (2018).
- ⁸⁸S. Habershon and D. E. Manolopoulos, *J. Chem. Phys.* **131**, 244518 (2009).
- ⁸⁹P. Huo, T. F. Miller, and D. F. Coker, *J. Chem. Phys.* **139**, 151103 (2013).
- ⁹⁰J. R. Duke and N. Ananth, *Faraday Discuss.* **195**, 253 (2016).
- ⁹¹J. E. Lawrence, T. Fletcher, L. P. Lindoy, and D. E. Manolopoulos, *J. Chem. Phys.* **151**, 114119 (2019).

- ⁹²J. E. Lawrence and D. E. Manolopoulos, *Faraday Discuss.* **221**, 9 (2020).
- ⁹³J.-L. Liao and G. A. Voth, *J. Phys. Chem. B* **106**, 8449 (2002).
- ⁹⁴G. Trenins and S. C. Althorpe, *J. Chem. Phys.* **149**, 014102 (2018).
- ⁹⁵K. A. Jung, P. E. Videla, and V. S. Batista, *J. Chem. Phys.* **151**, 034108 (2019).
- ⁹⁶K. A. Jung, P. E. Videla, and V. S. Batista, *J. Chem. Phys.* **153**, 124112 (2020).
- ⁹⁷J. Cao and G. A. Voth, *J. Chem. Phys.* **101**, 6168 (1994).
- ⁹⁸D. Bump, *GTM225: Lie Groups*, 2nd ed. (Springer, Switzerland, 2013).